SLAC – PUB – 3510
November 1984
(T/E)

EXPERIMENTAL METHODS OF HEAVY QUARK DETECTION*

T. HIMEL

Stanford Linear Accelerator Center
Stanford University, Stanford, California, 94305

Lecture presented at the 12th SLAC Summer Institute on Particle Physics,
Stanford, California, July 23 – August 3, 1984.

* Work supported by the Department of Energy, contract DE – AC03 – 76SF00515.

TABLE OF CONTENTS

1. Introduction

The purpose of these lectures is to explore the experimental methods of detecting heavy quarks. We will mainly consider searches for the top quark (charge = 2/3) and at times will mention how results for heavy bottom quarks (charge = -1/3) would differ.

Before we get too involved we should ask ourselves why we want to find top. The first reason is to see if it is there. To date there are five known quarks: u, d, c, s, b. They are conventionally arranged in doublets as shown below.

$$\begin{pmatrix} u \\ d \end{pmatrix} \quad \begin{pmatrix} c \\ s \end{pmatrix} \quad \begin{pmatrix} \Box \\ b \end{pmatrix}$$

Drawn like this, it appears there should be a sixth quark (top) to fill in the empty space.

Finding top and measuring its mass may help us find the pattern of fermion masses. So far we know that $m_e = 0.000511$, $m_\mu = 0.106$, $m_\tau = 1.784$, $m_u \approx 0.1$, $m_d \approx 0.1$, $m_s \approx 0.5$, $m_c \approx 1.5$, $m_b \approx 5.0$ GeV. With all these numbers we haven't been able to see the pattern and predict the top mass. Perhaps with knowledge of the top mass we will be able to see the pattern. After all, on the Scholastic Aptitude Test a student is given a series of four numbers and expected to predict the fifth. We already have five numbers in the series.

We will start our study of heavy quark detection by reviewing how the c and b quarks were found. Then we'll explain how things such as branching ratios and particle multiplicities change when going to heavier flavors. These changes require that new techniques be used in the search for top. We'll then mention what we already know about top from previous experiments and give some predictions of production cross sections.

Then we will delve into methods to look for top at the $\bar{p}p$ colliders at CERN and Fermilab. Rather than emphasizing exact numbers and giving optimum

methods of seeing it (i.e., a cookbook for an experimenter), we'll concentrate on giving a qualitative feeling of how things differ from c and b and what the problems are. From this you should understand why different techniques are used in looking for top, why the experimenters make the cuts they do and what backgrounds may cause problems.

The lectures will finish with a discussion of top search methods at SLC and LEP.

2. History: How c and b Were Found and Studied

The history contained in this lecture is far from complete. Hundreds of experiments have been done on the charm and bottom systems. Presented here are a biased sample. We have chosen experiments that illustrate techniques which might be used in top searches. In some cases we've shown the first experiment of a certain type, in others, a later experiment with higher statistics.

The story of charm starts in November 1974 with the "November revolution." Shown in Figures 1 and 2 are the results which launched the revolution. In a 30 GeV fixed target double arm spectrometer experiment the reaction $p + Be \rightarrow e^+e^-X$ was observed.[1] Shown in Fig. 1 is the e^+e^- mass spectrum. There is a prominent peak at 3.1 GeV. Its width of 20 MeV is consistent with the spectrometer's mass resolution. There is a very good signal-to-noise ratio and after several checks there was no doubt about the signal. The authors suggested the particle be called J.

Received by PRL the day after the preceding paper was one containing Fig. 2 showing the discovery of the ψ particle at 3.1 GeV by the SLAC-LBL group at SPEAR.[2] While the previous plot showed the e^+e^- invariant mass spectrum at a fixed beam energy, this one shows the cross section for $e^+e^- \rightarrow$ *hadrons* as a function of beam energy. The shape of the peak is consistent with the energy spread of the beam (0.56 MeV) folded with radiative processes; this is shown as

a dashed line in the figure. Hence they set a limit that FWHM of the resonance was less than 1.3 MeV. Note how big the signal is. The graph is on log paper. There is a cross section enhancement of over a factor of 100. Needless to say, these two experiments found the same particle which is now called the J/ψ. It is made up of a charm and an anticharm quark ($c\bar{c}$).

Knowing what to look for, the SLAC-LBL group found the ψ' (3685) 12 days later.[3] They scanned the beam energy of the e^+e^- storage ring in 1 MeV steps where the machine energy resolution was 1.2 MeV. They ran for three minutes at each point to measure the cross section. Shown in Fig. 3 are the data from the scan where the ψ' was found. In a more detailed rescan they measured the width of the ψ' to be less than 2.7 MeV.

While the J/ψ and ψ' were thought to contain charm quarks they still had a net charm quantum number of zero because they were $c\bar{c}$ pairs. To substantiate the charm model it was important to find particles with bare charm, such as $c\bar{u}$ or $c\bar{d}$, which have a non-zero charm quantum number. Evidence for such a particle, the D° was found at SPEAR 1-1/2 years after the original ψ discovery.[4] The reaction was

$$e^+e^- \rightarrow D^\circ X$$
$$\hookrightarrow K\pi \text{ or } K\pi\pi\pi$$

Shown in Fig. 4e is the signal for $D^\circ \rightarrow K\pi$. To obtain this they had to identify the π's and K's by using time-of-flight information (TOF). This reduced the background of combinations enough for the signal to show. They measured a mass of 1865 ± 15 MeV. To support the bare charm hypothesis they noted that recoiling opposite the D° was a system with an invariant mass greater than the D° mass. This made associated production of two charmed particles a likely explanation. Note that while there is a clear signal in Fig. 4, the signal:noise is only 1:1, much worse than for the J/ψ.

Continuing on in time we come to 1979, 4-1/2 years after the J/ψ. At this time the Lamp Shade Magnet experiment observed the Λ_c in pp collisions at the

ISR. Shown in Fig. 5 is their invariant mass plot of the $K^-p\pi^+$ system.[5] To see this signal they required both the K and p to be identified in Cerenkov counters. The mass resolution is quite good. The signal events all fall in one 20 MeV bin. It is clearly more difficult to see bare charm in pp than in e^+e^- collisions as indicated by the extra time it took to find it and the relatively poor signal/noise ratio.

We now come to our last example of charm detection. It was published in 1980 and is similar in many ways to the most promising top search method. Using the Big European Bubble Chamber with a Track Sensitive Target (BEBC+TST) in a 70 GeV π^- beam Barloutaud et al.,[6] looked for direct production of single electrons. These would be indicative of semileptonic decays of charmed particles. The main background came from asymmetric decays of π°'s, Dalitz pairs (where only one of the two electrons was detected) and $K^\pm \to \pi^\circ e^\pm \nu$. The later background was the most serious and was reduced by observation of the kink where the $K^\pm$ decayed. The p_T spectrum of the remaining electrons is displayed in Fig. 6. The statistics were low but the group claimed there was only one background event. As we will see in the next lecture, the most promising top search method looks for its semileptonic decay and the main background comes from semileptonic decays of bottom quarks just as the main background here came from semileptonic strange quark decays.

We will now go back in time to 1977 and cover the history of the bottom system. In doing so we will note how it differs from charm. This comparison will later help us understand why the top system is different.

Bottom was first observed, in the form of the Υ resonance in a 400 GeV fixed target experiment[7] in 1977. The reaction was $p + Cu$ or $Pt \to \mu^+\mu^- X$ where the $\mu^+\mu^-$ mass was reconstructed in a double arm spectrometer. The mass spectrum is shown in Fig. 7. The mass resolution is 200 MeV compared to 20 MeV for the charm case in Fig. 1. This worse resolution was mainly caused by the detection of muons instead of electrons. However it was necessary to use

muons in order to run the experiment at a high rate to get sufficient statistics (this experiment had a hadron absorber immediately after the target). Mainly because of the poorer mass resolution the signal:noise is only 1:1. Note that the background came from Drell-Yan production of muon pairs.

Later the same experiment with three times the statistics published more details of the Υ resonance.[8] The structure is shown in Fig. 8 and is consistent with 2 or 3 resonances with widths less than the experimental resolution. They had a total of 1200 signal events.

At the time of the Υ discovery there was no e^+e^- machine with sufficient energy to produce it. Because of the discovery the energy of DORIS was increased to allow its production. With the fairly accurate mass determinations from the Fermilab experiment it was then a simple matter to do a fine energy scan across the resonance while measuring the total cross section. The results are shown in Fig. 9.[9] The mass resolutions for the peaks are 7 and 12 MeV and are due to the energy spread of the e^+e^- beams.

The current status of the Υ system is illustrated in Fig. 10.[10] The data were taken by the CUSB collaboration at Cornell. There are four known peaks. The last one is wider than the machine resolution which was the first indication that it might decay to open bottom. Note that progress in the bottom system was helped enormously by the previous experience with charm.

The next step was to see evidence for bare bottom; that is, particles with a non-zero bottom quantum number with quark components such as $b\bar{u}$ or $b\bar{d}$. The hallmark of such a particle is that it cannot decay strongly or electromagnetically. It must decay weakly. Direct single electrons are a sign of this. In 1980 the CLEO collaboration[11] presented the results shown in Fig. 11 indicating that extra electrons were produced on the $\Upsilon(4S)$, the resonance which had a measurable width. This was indirect evidence for bare bottom production. A possible background was production and semileptonic decay of charm mesons. They eliminated this possibility by noting that the observed leptons had harder

momenta than those expected from charm decay (since charm is lighter than bottom, its decay products are softer). So once again a background for the heaviest flavor came from the next-to-heaviest flavor. They also presented evidence that extra $K^{\pm}$'s were produced on the $\Upsilon(4S)$. These presumably came from the quark decay chain $b \rightarrow c \rightarrow s$.

Complete reconstruction of specific decay modes of B mesons took much longer. It was not until 1983, four years after the Υ was seen in e^+e^- that CLEO published such results.[12] The high mass of the b quark allows it to have many decay modes each with a small branching ratio. Thus CLEO had to sum many different decay modes to get a significant signal. To reduce combinatorics, they used low multiplicity modes and required $K^{\pm}$'s to be positively identified by the detector. To improve the mass resolution they did beam constrained fits requiring the B meson energy to equal the beam energy. This resulted in a resolution of 8 MeV/c^2. The resulting mass spectrum is shown in Fig. 12. A signal is apparent at 5270 MeV but the statistics are limited and the background is non-negligible. Comparing this to Fig. 4 where the D° was observed we see that life gets harder as the quark mass increases.

3. What Do We Already Know About Top

Before discussing methods of detecting top it is useful to see what we already know about it. That way we have an idea of what we are trying to detect.

3.1 Lower Limits on the Top Mass

Since no new heavy quark state has been seen at Petra there are lower limits on new heavy quark masses. There are two methods used to set these limits. First, to look for a toponium peak, they have done a fine energy scan covering the top energy range of Petra. This scan was similar to that used to find the ψ'. The step size was 30 MeV while the storage ring's energy spread was 40 MeV. All the Petra experiments simultaneously measured the hadronic cross section.

The results from TASSO[13] are shown in Fig. 13. They set a limit that there could be no narrow peak with a size greater than 2/3 that expected for a charge 2/3 $Q\bar{Q}$ state. The statistics were too low to eliminate the possibility of a charge 1/3 $Q\bar{Q}$ state. Since they scanned up to 45.2 GeV, toponium must have a mass greater than that and m_t is greater than 22.5 GeV.

The second method was used to look for bare heavy quarks. Shown in Fig. 14 is the aplanarity distribution of hadronic events seen by TASSO. Aplanarity (A) is a measure of the shape of an event. Events where all the particles lie in a plane have $A = 0$; spherical events have $A = 1$. Events where two light quarks are produced have two back-to-back jets so most of the final particles lie near a single line; these events have $A \sim 0$. If one of the initial quarks radiates a gluon the final particles still lie near a plane so A is still near zero. The decay products of heavy quarks can go at large angles to the initial quark direction; these events are more spherical and have larger aplanarities. Hence use of the aplanarity helps separate events with heavy quark decays and improves the sensitivity. This is illustrated in Fig. 14 where the solid line shows the aplanarity distribution expected without a new heavy quark and the dashed line is the expectation with a 20 GeV top quark added. (Threshold effects were ignored in this Figure.) The data clearly supports the former one. Quantifying this, TASSO obtained limits that there were no new charge 2/3 (1/3) quarks with mass less than 22 (21) GeV.

3.2 Topless Models

Since no direct evidence has been seen for top, we will now consider models which do not have it, that is, topless models. The simplest topless model just puts bottom in a left handed singlet and it decays via the Z° or $W^\pm$:

$$\begin{pmatrix} u \\ d \end{pmatrix}_L \quad \begin{pmatrix} c \\ s \end{pmatrix}_L \quad (b)_L.$$

Just as a model with an s quark but no c quark would have strangeness-changing neutral currents, such a topless model would have flavor-changing neutral cur-

rents which would be visible in B meson decays. Kane and Peskin[14] have determined that any such model, independent of the addition of extra quark singlets must have

$$R \equiv \frac{\Gamma(B \to \ell^+\ell^- X)}{\Gamma(B \to \ell^+\nu X)} \geq 0.12.$$

This means there must be a certain fraction of B decays containing 2 leptons. This fraction has been measured at both Petra and CESR. The strictest limit comes from the CLEO collaboration which says that $R < 0.027$.[15] Hence, this class of topless models is not viable.

To avoid this problem people have devised topless models where the b has a new conserved quantum number so it can't decay via Z or W to lighter quarks. Then, since we know the b is not stable, they must invent a new interaction to allow it to decay, for example:

$b \to q$ higgs
$\hookrightarrow \tau^+\tau^-$
$\hookrightarrow$ leptons

These decays tend to have exotic products such as $b \to \ell_1\ell_2 q$ or $\ell q_1 q_2$ (where ℓ is a lepton and q is a light quark). CLEO has looked for the decay products predicted by a whole range of such models. The limits they set contradict this class of topless models.[16]

In summary, the top quark probably exists. We will now assume that the standard model with three quark doublets is correct.

3.3 LIMITS ON THE TOP QUARK MASS

An upper limit on m_t can be set by noting the equality of the charged and neutral current weak coupling.[17]

$$\rho \equiv \frac{G_{\text{neutral current}}}{G_{\text{charged current}}} = \frac{m_W^2}{m_Z^2 \cos^2 \theta_W}$$

This ratio is exactly 1 in a tree level calculation. Higher order corrections change the predicted value of ρ. In particular, the quark loop diagrams in Fig. 15 change ρ in a manner depending on m_t. From these calculations and the measured value of $\rho = 1.002 \pm 0.015$ the limit $m_t < 200$ GeV was determined.

It is also possible to set lower limits on the top mass. The method is discussed by Mark Wise in these proceedings so we will not go into detail here. The basic idea is that constraints on the generalized Cabibbo angles in the $K - M$ matrix are determined from many experimental measurements. The most important of these is the long b lifetime which indicates that θ_2 and θ_3 are small. One then calculates the amount of CP violation in the $K_L - K_S$ system.[18] This depends on the Cabbibo angles and the quark masses. Comparing this calculation to the measured value allows a lower limit to be set on m_t. This limit depends critically on the B lifetime. Using a value of τ_B one standard deviation below the world average gives $m_t > 42$ GeV. Going down two sigma gives $m_t > 25$ GeV which is not much stricter than the Petra limit of $m_t > 22$ GeV. Since B lifetime measurements are in their infancy and have large systematic errors and there is some uncertainty in the theoretical calculation, these lower limits on the top mass are not very conclusive.

4. Top Production Cross Sections at $\bar{p}p$ Colliders

The first step in detecting top is to produce it. To do this one needs a high enough center-of-mass energy ($\sqrt{s}$). As we have seen, PETRA's energy is insufficient to produce top. The Fermilab Tevatron running at 1000 GeV has $\sqrt{s} = 43$ GeV. As the $t\bar{t}$ threshold is above 44 GeV (from PETRA) this is insufficient. So, the first place we can hope to find top is at the $\bar{p}p$ colliders at CERN (the $S\bar{p}pS$ has $\sqrt{s} = 540$ GeV) and Fermilab ($\sqrt{s} = 2000$ GeV). CERN's machine turned on two years ago; Fermilab's will not turn on for another two years. The first e^+e^- machine with a $\sqrt{s}$ which may be high enough will be SLC which will turn on in early 1987.

Since the first place we can hope to detect top is in $\bar{p}p$ collisions, we will cover that first. This chapter will give the production rates and the following chapter some detection techniques. The production cross sections will be derived in a phenomenological manner – extrapolating from present energies. A more theoretical version is given in Kane's lectures in these proceedings.

First we will cover the production of toponium, the vector meson made of a $t\bar{t}$ pair. Shown in Fig. 16a are the scaled production cross sections of the lighter vector mesons as a function of $m/\sqrt{s}$ (the vector meson mass divided by the center-of-mass energy).[19] The data points lie near the solid curve which represents the scaling law:

$$\sigma_{pp\to V(q\bar{q})+X} = \frac{\Gamma_{3g}}{m^3} F(m/\sqrt{s}).$$

Here, Γ_{3g} is the total hadronic decay width (decay to 3 gluons) of the vector meson; it varies only slowly with energy. Note how the scaling works. If one increases both the quark mass and the center-of-mass energy by a factor of two, the cross section decreases by a factor of 8. At fixed energy the cross section falls even faster because $m/\sqrt{s}$ increases. The data and solid curve are for pp interactions. The dashed curve gives an estimate of the $\bar{p}p$ cross sections. The $\bar{p}p$

cross sections are higher because more antiquarks are available in a $\bar{p}$ than in a proton and as shown in Fig. 17 one of the production mechanisms for toponium involves the fusion of a quark and an antiquark.

The clearest signal for toponium would be its decay to lepton pairs just as it was in the b and c systems. The main background to this comes from Drell-Yan lepton pair production. Illustrated in Fig. 16b is the scaling law for this:

$$\sigma_{pp\to\ell^+\ell^- X} = \frac{1}{m^3_{\ell^+\ell^-}} F'(m_{\ell\ell}/\sqrt{s}).$$

Note the similarity between this and the scaling law for vector meson production. It turns out that F and F' are the same (they are determined by the momentum distribution of the partons in the proton), so the only difference is a factor of Γ_{3g} which decreases slowly as energy increases. Hence, the signal-to-noise ratio depends primarily on the branching ratio of the onium state to two leptons and on the mass resolution of the detector.

The branching ratio to two leptons is simply the decay width to two leptons, $\Gamma_{\ell\ell}$, divided by the total decay width. The scaling of $\Gamma_{\ell\ell}$ with quark mass is shown in Fig 18.[10] Roughly, $\Gamma_{\ell\ell} \sim e_q^2 \cdot 10$ keV where e_q is the quark charge. Hence for a fixed quark charge, the onium branching ratio to two leptons gradually decreases as mass increases because $\Gamma_{\ell\ell}$ stays constant and new decay modes open up making the total decay width increase. The net effect of all of this is that the signal-to-noise ratio gets poorer as the vector meson ($q\bar{q}$) mass increases. In fact, we have already seen that the S/N for the Υ was much worse than for the ψ. This resulted mainly from the smaller quark charge in the Υ and the poorer mass resolution of that experiment.

Shown in Fig. 19 are lepton pair production cross sections calculated on the basis of these scaling laws.[20] They are displayed for three energies corresponding to the ISR, the CERN $S\bar{p}pS$ and the Fermilab collider. The curves were normalized to ψ production at the ISR (shown as a triangular point). The measured Υ cross section lies close to the curve. Displayed as a solid line is the

cross section times branching ratio for vector meson production and decay into lepton pairs. The height of the curve indicates the total area a mass peak would have. The actual height of the peak depends on the detector's mass resolution. The dashed line shows the Drell-Yan cross section and the dot-dashed line shows the background from semileptonic decays of c and b quarks. Both of these background curves have been multiplied by the mass to give them the same units as the solid line. To get the signal-to-noise ratio from these plots, just take the height of the signal curve divided by the height of the background curve divided by the experimental mass resolution (e.g., 0.01 if the experiment has a 1% mass resolution). The S/N decreases with increasing mass and energy for the reasons explained above.

While the S/N is worse, it may still be possible to see a toponium signal if enough events are collected. Typical integrated luminosities collected by experiments are 10^9, 10^4 and 10^2 nb^{-1} by fixed target, ISR, and $\bar{p}p$ collider experiments, respectively. The scale on the right of Fig. 19 indicates the number of events produced per 100 nb^{-1} of integrated luminosity, that being typical of a $\bar{p}p$ collider run. Less than one event is expected, even for a 45 GeV/c^2 toponium mass (the minimum allowed by PETRA). The plots show pp cross sections; the $\bar{p}p$ cross sections will be somewhat higher, but not enough higher to allow a signal to be observed. What has been (for c and b) the easiest way to detect a new flavor will not work for top.

Since toponium will not be visible at the $\bar{p}p$ colliders we now go on to production of open top. There are several ways open top can be produced. We will proceed from the straight-forward to the uncertain calculation.

If the top quark is lighter than the W boson, bare top can be produced in the decay $W^+ \to t\bar{b}$ as illustrated in Fig. 20. The rate for this is given by[21]

$$\frac{\Gamma(W \to t\bar{b})}{\Gamma(W \to e\nu)} = 3\left|U_{tb}^2\right|(1-x)\left(1-\frac{1}{2}x-\frac{1}{2}x^2\right)$$

where $x = m_t^2/m_W^2$ and U_{tb} is an element of the K-M matrix which is approx-

imately 1. As $\sigma\ (\bar{p}p \rightarrow W \rightarrow e\nu)$ has been measured and agrees well with calculation, the cross section estimate shown as the solid line in Fig. 21 is fairly reliable.

Open top can be produced by the same quark or gluon fusion diagrams that allowed toponium production (Fig. 17). Although the diagrams are the same, the cross section is higher because the t and $\bar{t}$ don't have to stick together as they do in toponium. Shown as a dashed line in Fig. 21 are the results of a calculation[22] of this cross section. It has an uncertainty of a factor of 2 or 3. Note that for $m_t \lesssim 35$ GeV this cross section is higher than that from W decay but the events lack the nice feature of containing the decay products of a W.

While the above mechanisms produce top primarily in the central region, there are other mechanisms which would produce it primarily in the forward region. Models which do this are the simple diffractive model,[22] flavor excitation[23] and intrinsic charm.[24] These models were developed mainly to explain observed forward production of charm. Unfortunately the interpretations of the experiments are complicated by model dependencies of cross sections and extrapolations from a limited acceptance to the full solid angle. The models based on these experiments necessarily have large (factor of 10 or larger) errors. The prediction of the diffractive model is shown as the dotted line in Fig. 21. Because of the uncertainty of the forward production cross sections, we will not use them in the remainder of these lectures.

So far we have been looking at total production cross sections. We have seen that higher quark masses have smaller cross sections. The problem this causes is made clear in Fig. 22 which shows the differential cross section for heavy quark production (from $q\bar{q}$ and gluon-gluon fusion).[25] There are many more b and c quarks produced than t quarks. There are still more gluon jets. Sorting a top signal out from this background will not be easy.

5. Top Detection Techniques at the $\bar{p}p$ Collider

The methods of separating top decays from the background all depend on distinctive features of top decays. These features are all due to the large top mass. Top mesons usually decay hadronically. This decay will result in a jet much broader (because of the high t mass) than the typical light quark or gluon jet. With about a 10% branching ratio top will decay semileptonically as shown in Fig. 23. Another 10% of the time it will decay with a μ^+ in the final state. Because of the large t mass, these leptons will be well separated from the jet caused by the b decay and can be used as a signature for top decay. For most purposes e's and μ's are interchangeable so in this chapter we will use e, μ and ℓ (for lepton) interchangeably.

5.1 Search for Exclusive Decay Modes

First we will consider the reconstruction of exclusive top decay modes, that is, the detection of all the decay products of a top meson and calculation of the invariant mass. As was shown in Fig. 21 only about 200 t's are produced for the typical integrated luminosity of 100 nb^{-1}. Unfortunately the top decay chain is quite complex: $t \to b \to c \to s$. At each of the 3 steps in this decay chain there is only about a 5% branching ratio to go to a few simple exclusive states. This leaves only 0.02 signal events – clearly the statistics are insufficient. Even with much more integrated luminosity the task would be very difficult. Remember how much more difficult it was to isolate bottom meson decays than charm meson decays. As the mass increases, the number of available decay modes increases, branching ratios decrease and multiplicities increase causing combinatoric problems (in each event there are many combinations of particles which could come from a top decay). Taken all together, detection of exclusive top decays looks hopeless.

5.2 Jet Size and Shape Analysis

Perhaps one can find evidence for top by looking inclusively at all its hadronic decays. The large top mass should make top events look different than events with only light quarks or gluons. Typical $p\bar{p}$ events that have a large transverse energy consist of two narrow back-to-back jets of particles. Each jet results from the fragmentation of an initial high p_T quark or gluon. Because of its large mass the jet resulting from a top quark should be broader. The main background to this comes from the bremsstrahlung of hard gluons from light quark or gluon jets. This extra gluon can result in a third jet in the event or can be merged with the initial jet resulting in a single broad jet. Unfortunately the strong coupling constant, α_s, is not small so this type of bremsstrahlung happens quite often. In events with two 20 GeV/c jets, 29% have a third jet over 5 GeV/c and 5% have one over 8 GeV/c.[26] So a fair fraction of the time jets can be broadened by gluon bremsstrahlung.

To make matters worse, top jets are not as massive as one might hope. Shown in Fig. 24 is a result of a Monte-Carlo study of top decay.[27] Top quarks of 35 GeV mass and 50 GeV/c momentum were generated and fragmented. The invariant masses of all the decay products entering a 45° cone centered on the jet axis were reconstructed. The figure shows that the resulting reconstructed mass has a wide distribution centered on 20 GeV rather than 35 GeV. The top is so massive that some of its decay products go backwards and are not used in the reconstructed jet mass. As the full top mass is not reconstructed, it is harder to distinguish from light quark and gluon jets then one would naively expect.

A thorough Monte-Carlo comparison of top and QCD jets and methods of discriminating between them has been done by Ballocchi and Odorico[27] They compared angular widths, masses, particle multiplicities, shapes and their correlations. They concluded that top jets cannot be unambiguously identified by their jet characteristics because the fluctuations in jet fragmentation are larger than the differences between top and gluon jets. Perhaps this separation technique

can be used to supplement another identification scheme.

5.3 SEMILEPTONIC DECAYS

So far we have investigated several heavy flavor detection methods which worked quite well for c and b but will not work for top. We now go on to the most promising method for top detection at the $p\bar{p}$ collider: observation of its semileptonic decays.

The basic problem is illustrated in Fig. 25 which shows the transverse momentum spectrum, p_{eT}, of electrons from various sources.[28] The solid curves show the electron signal from top whose source is $W \rightarrow t\bar{b}$. Curves are shown for top masses of 25 and 40 GeV. The dashed curves give the electron spectra from strong top production and the dot-dashed curves show background spectra from $b\bar{b}$ and $c\bar{c}$ production. Finally, the highest curve shows the differential jet cross section. Since there are as many electrons from b decays as from t decays, it is clear we will need a way to distinguish the two. Also, very good rejection against jets faking electrons in the detector will be needed because there are 10^6 more jets than electrons. One also notes that the spectra fall rapidly with p_T so it is important for experiments to utilize electrons of as low a p_T as possible. Requiring $p_T > 8$ GeV/c loses half the electrons; requiring $p_T > 15$ GeV/c loses 80% of them. With an integrated luminosity of 100 nb^{-1} there will only be 2 events with $p_{eT} > 15$ GeV/c coming from W decays. Since the number of signal events expected is so low, a very good signal-to-noise is needed to obtain a significant signal. This last requirement keeps experiments from using low p_T electrons as background rejection is much worse at low p_T.

To see how top decays can be separated from the backgrounds, we will now investigate the kinematics of the decay. Shown in Fig. 26 is a sketch of an event where $W \rightarrow \bar{t}b$ and the $\bar{t}$ semileptonically.[29] Note that the b quark from the W decay is relatively light and has a high momentum so it makes a narrow, well collimated jet. The $\bar{t}$ decays to an electron, neutrino and a b quark. Since

the $\bar{t}$ is so heavy these are well separated and the electron will normally not be back-to-back with the b jet. So the top signature would include a hard narrow jet with a softer jet, a well separated electron (or muon) and some missing p_T (the neutrino).

The kinematics illustrated in Fig. 27 demonstrate the basis for cuts that can be used to separate a $W \rightarrow t\bar{b}$ signal from $b\bar{b}$ background. Shown in the center column are three ways that a heavy quark (b or t) could semileptonically decay. They are displayed in the rest frame of the heavy quark. The left column shows the same events boosted to the lab frame as they would be for a $M = 35$ GeV top quark coming from a W decay. The right column shows a similar b decay in the lab frame. Note that in the b decay the opening angle between the electron and the charm jet is always small ($< 16°$) while in the top decay this angle is larger. In b decay the electron is usually accompanied by particles from the nearby jet while in t decays it is often isolated. This forms the basis for a very important cut. Note in the bottom right of the figure that in b decay it is possible for the charm jet to be so soft (4 GeV/c) that a detector may miss it. Events like this that are accompanied by an extra jet from QCD bremsstrahlung form a source of background for top.

Now that we have some ideas of the cuts necessary to isolate a top signal, how do we get a mass peak or prove we have a signal in some way? One possibility is to histogram the momentum of the highest energy jet in the selected events. The p_T of b jets where $W \rightarrow \bar{t}b$ are expected to have a Jacobian distribution as illustrated in Fig. 28.[29] With sufficient statistics the position of the peak could be used to determine the top mass. The peak will, of course, be smeared out by the hadronic energy resolution of the detector which is typically 3 GeV/c^2.

It is also possible to get an estimate of the top mass directly from its decay products. Lack of knowledge about the neutrino momentum makes this difficult. The lepton momentum spectrum does not give much information about the top mass; it depends as much on p_T of the t as on the top mass. Experiments can get

an estimate of the p_T of the neutrino by assuming it balances the total measured p_T of the event. The longitudinal momentum, p_L (momentum parallel to the beam line), of the neutrino cannot be determined because fragments of the initial protons with unknown p_L escape down the beam pipe. Since p_L is unknown we ignore it and define the transverse mass of the electron and neutrino:

$$M_T^2(e\nu) \equiv (|P_{e_T}| + |P_{\nu_T}|)^2 - (\vec{P}_{e_T} + \vec{P}_{\nu_T})^2.$$

If the b jet (from $t \rightarrow e\nu b$) is seen, one can get a more precise mass estimate by first adding its 4-momentum to that of the electron and then forming the transverse mass of that with the neutrino. This transverse mass has the symbol: $M_T(be,\nu)$. Note that these transverse mass calculations work whether the t is produced via $W \rightarrow t\bar{b}$ or by QCD production of $t\bar{t}$.

Shown in Fig. 29 are Monte Carlo calculations of these transverse mass distributions.[30] The cluster transverse mass has a nice peak which is well separated from the $b\bar{b}$ background. The cuts used in selecting events for these plots will be explained later. For the moment it is only important to note that we can measure a quantity closely related to the heavy quark mass and it can be used to confirm the presence of a signal as well as measure the mass.

Having found a way to measure the mass, we will now investigate how to separate the signal from the background. This will be based on the previously explained decay kinematics. First one must require a relatively large p_T of the electron. This helps keep hadrons from faking electrons in the detector. Unfortunately a high p_{e_T} cut considerably reduces the acceptance for top. Cuts will typically vary between 8 and 20 GeV/c. The optimum cut depends on the detector's hadron rejection capabilities. Most of the plots shown here use a cut of 15 GeV/c.

As noted earlier, because of the large top mass the electron tends to be well separated from the other top decay products. Shown in Fig. 30 is a Monte-Carlo calculation of this effect.[31] It shows the amount of energy contained within a

$\pm 30°$ azimuthal angle of the electron. There is much less energy near the lepton from top decay than from b or c decay. So a cut on this, often called an isolation cut, will improve the signal-to-noise in a top analysis.

Semileptonic decays have not only an electron in the final state but also a neutrino. In identifying W decays the requirement of evidence of a neutrino was a powerful tool in reducing the background.[32] Perhaps a similar technique could help identify top. The collider experiments cannot directly detect neutrinos; they measure the total transverse momentum and assume a neutrino balances it. This measurement which is made with hadronic calorimeters has an error of about 5 GeV/c. This error is small compared to the momentum of a neutrino from W decay but not negligible compared to the momentum of a neutrino from top decay. Top decay is further complicated by the fact that its decay products (a b quark and then c quark) can decay semileptonically emitting more neutrinos. All of these problems taken together: the low neutrino momentum, the large measurement error, and multiple neutrino emission make missing p_T cuts nearly useless in top analyses.[33]

It should be emphasized that the plots shown are all the results of Monte Carlo calculations and depend on the assumptions used by the authors. Many early calculations were over simplified, e.g. multiple neutrino emission or gluon bremsstrahlung or detector resolution were neglected, and resulted in unrealistic answers. Figures 31 and 32 show the results of two calculations done by the same people first without and then with gluon bremsstrahlung.[34] Plotted are the p_T distributions of leptons from t and b decay. In the first plot it looks like requiring $p_T > 8$ GeV/c would eliminate all background from b decays. In the second more refined calculation there are higher momentum leptons from the b decay resulting in a residual background. The full leptonic momentum spectrum did not actually get harder. Both plots were made with a cut requiring the presence of at least two 8 GeV/c jets. The addition of gluon bremsstrahlung created extra jets and allowed more background events to pass this cut. The moral of the story is that these theoretically based Monte Carlo calculations can be used as guidelines in

an experimental analysis but internal experimental checks are needed to be sure of a signal.

Keeping this in mind we return to the transverse mass distribution in Fig. 29. It was made requiring a lepton with $p_T > 8$ GeV/c, at least two jets with $p_T > 8$ GeV/c and an isolation cut requiring there to be less than 3 GeV/c in a 30° cone around the lepton. It looks like a top signal should be easily distinguishable from the $b\bar{b}$ background. Of course, the expected statistics of less than two events and the possibilities of other types of backgrounds keep the experimental analysis from being totally trivial.

So far we have mainly considered background caused by leptons from semileptonic b decays. There are other possible backgrounds. Electrons can come from photon conversions in the beampipe or from Dalitz decays of π^0's; these electrons tend to be inside jets and are thus removed by the isolation cut. Muons can come from π and K decays. An electron signal can be mimicked in a detector by the overlap of a π^+ and a π^0. Electrons with a few GeV/c of nearby π^0's may pass the isolation cut in reality while they failed it in the Monte Carlo. With all of these possible background sources, many of which are detector dependent, it is clear that one must estimate the background from the data.

Another potential background source comes from normal QCD production of light quark or gluon jets. A comparison of how a $b\bar{b}$ event and a gluon event can simulate a top event is given in Fig. 33. Remember that the signature we are using for top is two jets and an isolated electron. A $b\bar{b}$ event can produce this by having the b bremsstrahlung a gluon at large angle and then semileptonically decay. If the charmed jet from that decay is soft and thus unobserved, a top event is mimicked. A gg event can mimic top if one of the gluons bremsstrahlungs another and one of the gluon jets simulates an isolated electron in the detector. You can see that these two processes are quite similar. The only difference is that the $b\bar{b}$ events already have an electron from a semileptonic decay while the detector must identify a gluon jet as an electron for a gg event to simulate

top. This misidentification is improbable but remember the very large number of produced two-jet events shown in Fig. 25.

The backgrounds can be very treacherous. Not only are there many different sources, but background events will tend to peak at a fairly high mass. Low mass events are removed by the kinematic cuts requiring minimum p_T's for the electron and jets. There are very few high mass events because production cross sections fall off exponentially with p_T. The result is a broad peak in the background at intermediate mass. The combination of expecting a broad peak for the signal, having the background peak and having very limited statistics, makes it extremely important to have a realistic background estimate.

A good way to obtain this background estimate is to use the data itself. The top analysis we have been describing consists of two parts: the identification of an isolated lepton and requirements on the topology of the events (e.g., two jets with $p_T > 8$ GeV/c). By assuming the background rejection powers of these two parts are independent, we can estimate the amount of remaining background in the following way. Using two jet events we can measure how often jets (including gluon, light and heavy quark jets) are misidentified as electrons. This is done by assuming that events with a jet opposite an identified electron actually had two jets where one was misidentified. This misidentification probability may be a function of the p_T of the jet. We then take jet events (with no lepton cuts) which satisfy the topology cuts and, treating one of the jets as a lepton, histogram the physics distribution in which we are interested (e.g., $m_T(e\nu)$). Each entry in the histogram is weighted by the probability that the jet in that event could be misidentified as an electron. The resulting histogram is the background estimate. This background calculation should be checked by seeing if it agrees in shape and magnitude with events one knows are background. If the signal distribution is so clean that there are not enough background events with which to compare, one can loosen the lepton cuts to generate enough background events to allow comparison.

Perhaps an example will clarify this method of calculating the background. Shown in Fig. 34 are p_{e_T} distributions from the UA2 W analysis.[35] The histograms show the p_T distribution of events which passed all electron cuts. The curves are background estimates. The three plots represent different topologies: an electron with no jet, an electron with a jet opposite it, and an electron with a jet which is not opposite it. It was assumed that all the events in the second plot were background, that is, the identified electron was really a jet which faked an electron in the detector (via Dalitz decay or $\pi^+\pi^\circ$ overlap, etc.). With that assumption and a histogram of the p_T distribution of jets in two jet events it was calculated that there was a 1 in 50,000 chance that a jet was identified as an electron by UA2. (A technical detail: UA2 did not actually use all jet events in this analysis; they were not all on tape; only jets which passed some loose electron cuts were used.) This misidentification probability turned out to be independent of p_T for $p_T > 15$ GeV/c. Having used Fig. 34b to determine the normalization, the background curve for Fig. 34a was obtained by histogramming the p_T of the jet in events with a single jet and dividing by 50,000. Similarly for Fig. 34c the p_T's of jets in events with two jets that were not back-to-back were histogrammed and divided by 50,000 to get the background curve. The high p_T electrons came from $W \rightarrow e\nu$. At lower p_T the background dominates and the data agree well in both magnitude and shape with the background estimate. So this simple method with very few assumptions gives quite accurate background estimates in the W analysis. The same method should also work in a top search.

In summary, a few semileptonic top decays might be expected at the $p\bar{p}$ collider. The high quark mass can be used to separate the signal from background, but since the statistics are low and the background sources numerous, one must make very careful background estimates.

6. Top Searches in e^+e^- Collisions

So far we have studied top detection techniques for the $p\bar{p}$ collider. We have seen that it may be possible but difficult to observe it there. Certainly it is impossible to measure many of its properties. At best one can measure its mass and cross section times branching ratios for one or two decay modes. We will now investigate how top can be observed at e^+e^- colliders where historically the wealth of information on heavy flavors has been obtained.

There are two e^+e^- machines being built which may be able to produce top: the SLC at SLAC and LEP at CERN. We are ignoring Japan's Tristan to keep things simple. The SLC is scheduled to produce beams for physics purposes early in 1987 while LEP should turn on in early 1989. SLC's design luminosity varies only slowly with energy and is $\mathcal{L} \approx 6 \times 10^{30}\ cm^{-2}\ sec^{-1}$. LEP's design peak luminosity is $\mathcal{L} \approx 2 \times 10^{31}\ cm^{-2}\ sec^{-1}$ at $E_{cm} = 70$ GeV/c^2 and $\mathcal{L} \approx 4 \times 10^{31}$ at $E_{cm} = M_{Z^\circ}$. As LEP must be periodically refilled, its peak luminosity must be derated by a factor of about 3 to get an average luminosity. Then since no e^+e^- machine has ever obtained its design luminosity in the first year, we will derate the luminosities of both machines by another factor of 6 to give an even $\mathcal{L} = 10^{30}\ cm^{-2}\ sec^{-1}$ for both machines. This luminosity will be used in calculating event rates. If you are more optimistic or pessimistic than we are, you may scale the event rates given here accordingly.

6.1 Production Cross Sections

Heavy quark production cross sections are known much more accurately for e^+e^- interactions than for $p\bar{p}$. For this example we will assume a top quark mass of 35 GeV/c^2. The $\mu^+\mu^-$ production cross section is

$$\sigma_{\mu\mu} = \frac{4\pi\alpha^2}{3s} = \frac{86.8\ nb}{s(GeV^2)}$$

where s is the square of the center-of-mass energy. This gives $\sigma_{\mu\mu} = 0.018$ nb at $\sqrt{s} = 70$ GeV. The total hadron production cross section is about four times

this giving 6 hadronic events per day at $\mathcal{L} = 10^{30}$. If $\sqrt{s}$ is well above open top threshold, the cross section for open top production will be $4/3\ \sigma_{\mu\mu}$. This would result in two open top events per day.

The production cross section for toponium is also well known. If an energy scan is done (like for the ψ and Υ) to measure the total hadronic cross section, the area of the toponium peak would be $\frac{6\pi^2}{m_{t\bar{t}}^2}\Gamma_{ee}\ B_{had} = 0.014$ nb GeV. As the width of toponium is expected to be much less than the accelerator's energy resolution, the width and therefore the height of the peak depends on the energy spread of the accelerator. At LEP and SLC the designed energy resolutions are 0.1% and 0.5% , respectively. At energies below the Z° the resolution of the SLC can be improved by tuning the linear accelerator properly. With a resolution of 0.1% and $\mathcal{L} = 10^{30}$ five toponium events per day are expected at the peak of a 70 GeV/c^2 toponium. This should be compared to six continuum events. It would take two days to get a three standard deviation signal. If a scan is done with a step size of the machines energy resolution, 0.1 GeV, it will take 20 days to scan each GeV. Unless there is a very good estimate of the toponium mass, it will take a long time to find it this way. There must be a better way.

The method used at PETRA to see if they were above open top threshold will also work at SLC and LEP. Shown in Fig. 35 is the distribution of aplanarity expected for light quarks and for a 30 GeV/c^2 top quark.[36] Since the t quark is heavy its decay products go out at large angles and do not lie in a plane. This results in larger aplanarities than those from light quark decays. So the aplanarity distribution gives a good means to tell if one is above top threshold. It is possible to use this method to find the threshold for open top. If you run at an energy above top threshold for about five days then ten top events will be produced. It is then fairly certain that you would see one with a large aplanarity. If you do not, you are below top threshold and you try again at a higher energy. If you do, you are above top threshold and you run at lower energy to zero in on the threshold. In this way a binary search can be done to locate the threshold within 1 GeV/c in six 5-day runs. The runs near threshold will actually require

higher statistics because the top production cross section is smaller there.

There may be a still easier way to find top at an e^+e^- collider. If the top quark mass is less than 45 GeV/c^2, top mesons will be produced copiously in Z° decays. Shown in Fig. 36 is how t quark production depends on the t mass.[37] The normalization is that a light t quark will be produced in 14% of Z° decays. Now with $\mathcal{L} = 10^{30}$ one expects 6000 Z° events/day. For $m_t = 35$ GeV/c^2 250 tops would be produced each day. At last we have a reasonable production rate.

How can these top events (identified by their large aplanarity) be used to measure the top quark mass? We can try calculating the jet mass, the invariant mass of all particles in the top jet. Shown in Fig. 37 is a Monte Carlo calculation of this for two different top masses.[37] The distributions are not very different which indicates that this method cannot be used to measure the top mass. The problem here is the same as it was in $p\bar{p}$ production of top. The quark is so heavy that some of its decay products go backwards and are not included in the jet. Thus, the calculated mass is inaccurate.

A method which will work better uses the leptons from semileptonic top decays. Their momenta transverse to the jet axis give a crude measure of the top mass. Shown in Fig. 38 is a Monte Carlo of this spectrum for two different top masses.[38] The endpoint of the spectrum clearly depends on the mass. It takes high statistics to do this measurement, but remember that 250 t's per day could be produced at the Z° and experimenters will be running on the Z° for many other reasons. So this method of obtaining the top mass does not require any special runs.

7. Complex Scenarios

So far we have concentrated on searches for a fairly specific heavy quark, namely with charge $+2/3$ and mass between 22 and 45 GeV/c^2. We now consider scenarios with a charge $1/3$ quark or a heavier t quark.

What if there is a new charge $1/3$ quark, b', with mass less than top? In many respects it will appear just like a top quark (charge $= 2/3$). Its production rates in hadronic interaction, decays and detection methods would be about the same as for top. Its e^+e^- production cross section would be down a factor of four because it is proportional to the charge squared. It probably would not be produced in W decay because its charge $2/3$ partner would be too massive. When a heavy quark is discovered this may allow one to distinguish between the two charges.

It is possible that both top and a new charge $1/3$ quark are accessible with present accelerators. This complex case would be quite difficult to untangle. Shown in Fig. 39 is a calculation of the transverse cluster mass distribution for the case of two new quarks with 30 and 40 GeV/c^2 masses.[39] Recalling that only a few events are expected with present day integrated luminosities, it will be a long time before sufficient statistics are available to unravel a complex case like this.

If top is much heavier than we have been considering, its detection becomes very difficult. With a mass greater than 45 GeV/c^2 it would not be produced in Z° decays. This makes its detection at the new generation of e^+e^- machines unlikely. Shown in Fig. 40 are the calculated production cross sections for heavy quarks at the two $p\bar{p}$ collider energies.[40] With integrated luminosities an order of magnitude higher than we have now, it may be possible to detect quarks with masses up to 100 GeV/c^2.

8. Summary

By comparing how b and c were observed we saw that the heavier quark was more difficult to detect. For various reasons the signal was smaller and the signal-to-noise worse. This trend is expected to continue when searching for the still heavier top quark. In fact many detection techniques which worked well for bottom and charm are not viable for top.

For masses less than about 60 GeV/c^2 top should be visible at the CERN $S\bar{p}pS$. For larger masses the higher energy of the Fermilab Tevatron will be necessary. At both machines semileptonic decays are the most promising tag. There are background rejection techniques which should result in a fairly clean signal. As there are many possible background sources it is important to carefully estimate the residual background from the data itself.

At e^+e^- machines top will be copiously produced in Z° decays if $M_t < M_{Z^\circ}/2$. In this case it is possible to estimate its mass and study its decay modes.

REFERENCES

1. J. J. Aubert et. al., Phys. Rev. Lett. 33, 1404 (1974).
2. J.-F. Augustin et. al., Phys. Rev. Lett. 33, 1406 (1974).
3. G. S. Abrams et. al., Phys. Rev. Lett. 33, 1453 (1974).
4. G. Goldhaber et. al., Phys. Rev. Lett. 37, 255 (1976).
5. K. L. Giboni et. al., Phys. Lett. 85B (1979).
6. R. Barloutaud et. al., Nucl. Phys. B179, 25 (1980).
7. S. W. Herb et. al., Phys. Rev. Lett. 39, 252 (1977).
8. W. R. Innes et. al., Phys. Rev. Lett. 39, 1240 (1977).
9. J. K. Bienlein et. al., Phys. Lett. 78B, 360 (1978).
10. M G. D. Gilchriese, Proceedings of the 11th SLAC Summer Institute on Particle Physics, July 1983. SLAC-Report-267.
11. E. H. Thorndike Proceedings of the 20th International Conference on High Energy Physics, Madison, Wisconsin (1980).
12. S. Behrends et. al., Phys. Rev. Lett. 50, 881 (1983).
13. M. Althoff et. al., Phys. Lett. 138B, 441 (1984).
14. G. L. Kane and M. E. Peskin, Nucl. Phys. B195, 29 (1982).
15. P. Avery et. al., Preprint: CLNS-84/612.
16. A. Chen et. al., Phys. Lett. 122B, 317 (1983).
17. L. Maiani, Proceedings of the 21st International Conference on High Energy Physics at Paris (1982); M. Veltman, Nucl. Phys. B123, 89 (1977).
18. P. H. Ginspurg, S. L. Glashow and M. B. Wise, Phys. Rev. Lett. 50, 1415 (1983).
19. D. M. Scott, Proceedings of the 20th International Conference on High Energy Physics, Madison, Wisconsin, 1980.

20. S. Pakvasa et. al., Phys. Rev. D20, 2862 (1979).

21. V. Barger, A. D. Martin and R. J. N. Phillips, Phys. Lett. 125B, 343 (1983).

22. D. M. Scott, Proceedings of the Proton-Antiproton Collider Physics Conference, Madison, Wisconsin, 1981.

23. V. Barger, F. Halzen and W. Y. Keung, Phys. Rev. D25, 112 (1982).

24. S. J. Brodsky and C. Peterson, Phys. Rev. D23, 2745 (1981).

25. F. Halzen and D. M. Scott, Phys. Lett. 129B, 341 (1983).

26. L. Fayard, Thesis, LAL 83/82 (1983).

27. G. Ballocchi and R. Odorico, Nucl. Phys. B229, 1 (1983).

28. R. Odorico, preprint PRINT-83-0965.

29. V. Barger, A. D. Martin, and R. J. N. Phillips, Phys. Lett. 125B, 343 (1983).

30. V. Barger, Phys. Rev. D29, 1923, (1984).

31. R. Odorico Preprint: PRINT-83-0765.

32. G. Arnison et. al., Phys. Lett. 122B, 103 (1983); M. Banner et. al., Phys. Lett. 122B, 476 (1983).

33. G. Ballocchi and R. Odorico, Phys. Lett. 136B, 126 (1984).

34. V. Barger et. al., Phys. Rev. D29, 887 (1984); V. Barger et. al., Phys. Rev. D29, 1923 (1984).

35. P. Bagnaia et. al., Z. Phys. C. Particles and Fields 24, 1 (1984).

36. J. Dorfan, Proceedings of the 10th SLAC Summer Institute on Particle Physics (1982), SLAC-Report-259, p. 137.

37. Proceedings of the SLC Workshop on Experimental Uses of the SLAC Linear Collider, SLAC-Report-247 (1982).

38. Proposal for the Mark II at SLC, CALT-68-1015 (1983).

39. V. Barger and R. J. N. Phillips, Preprint: MAD-PH-159 (1984).

40. M. Dechantsteiter et. al., Phys. Rev. D25, 258 (1982).

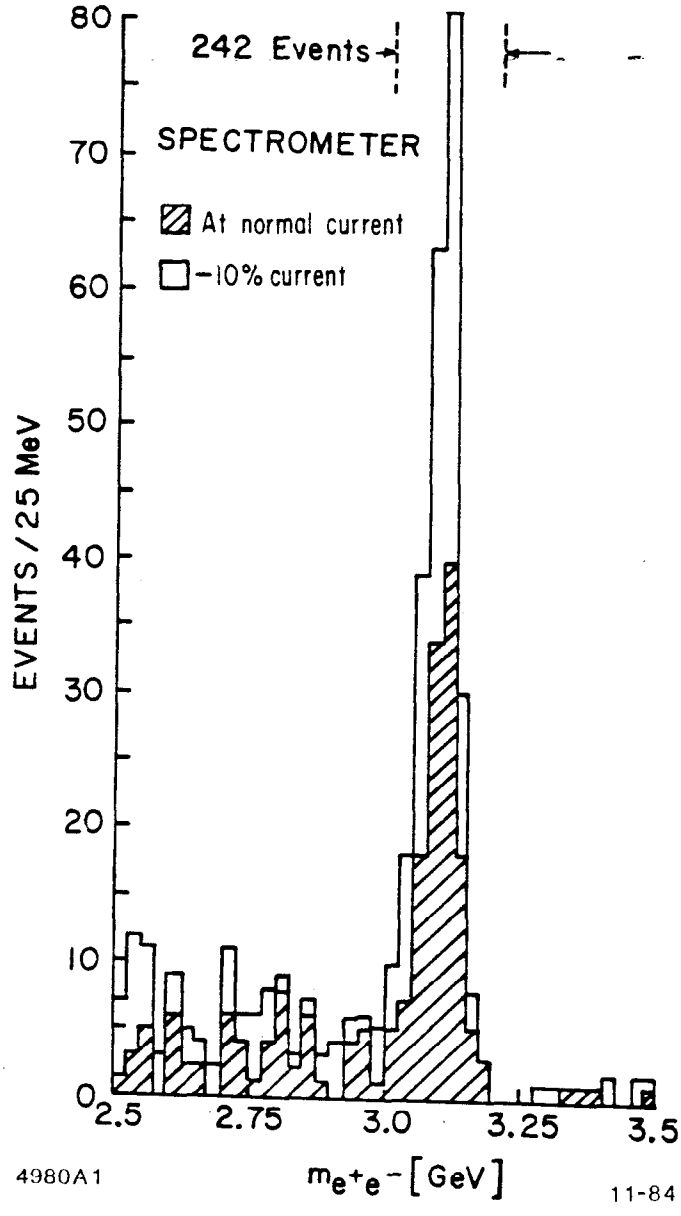

Fig. 1. Invariant mass spectrum of e^+e^- pairs seen in $p + Be \rightarrow e^+e^-X$. The J is discovered.

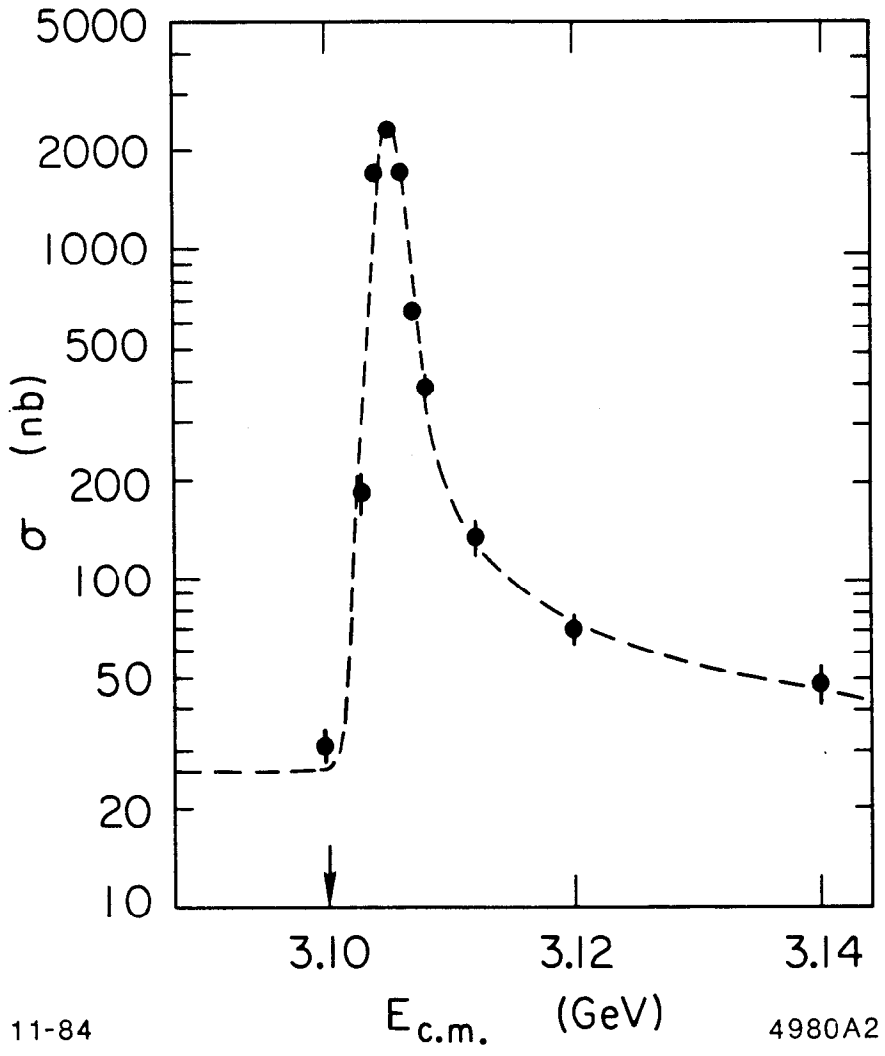

Fig. 2. Total cross section for $e^+e^- \rightarrow$ hadrons. The ψ is discovered.

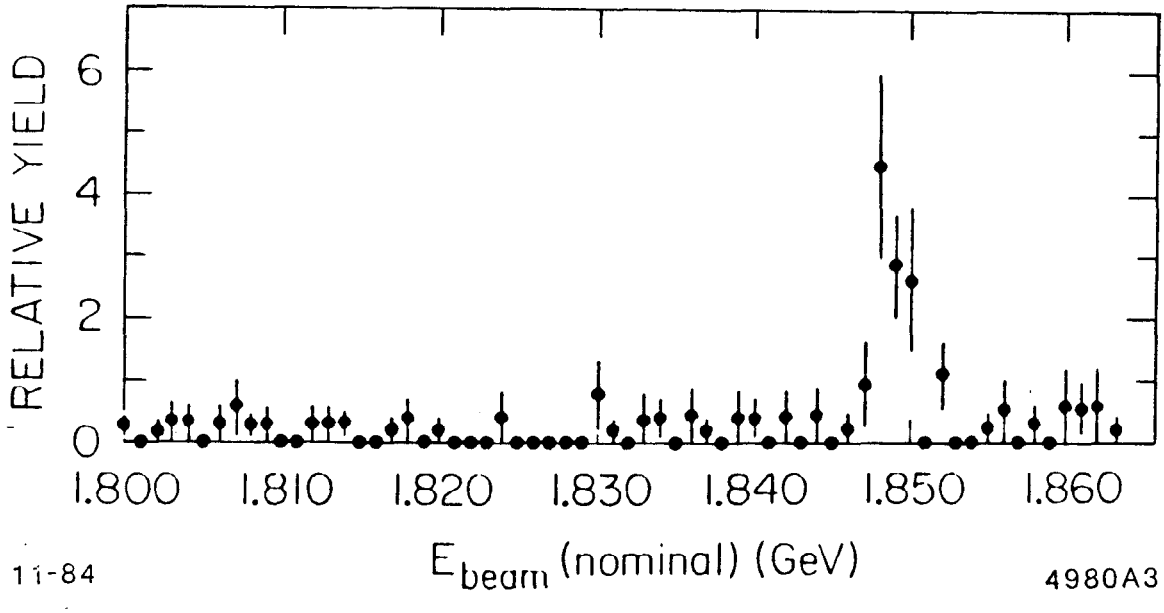

Fig. 3. Energy scan of total cross section for $e^+e^- \rightarrow$ hadrons. The ψ' is discovered.

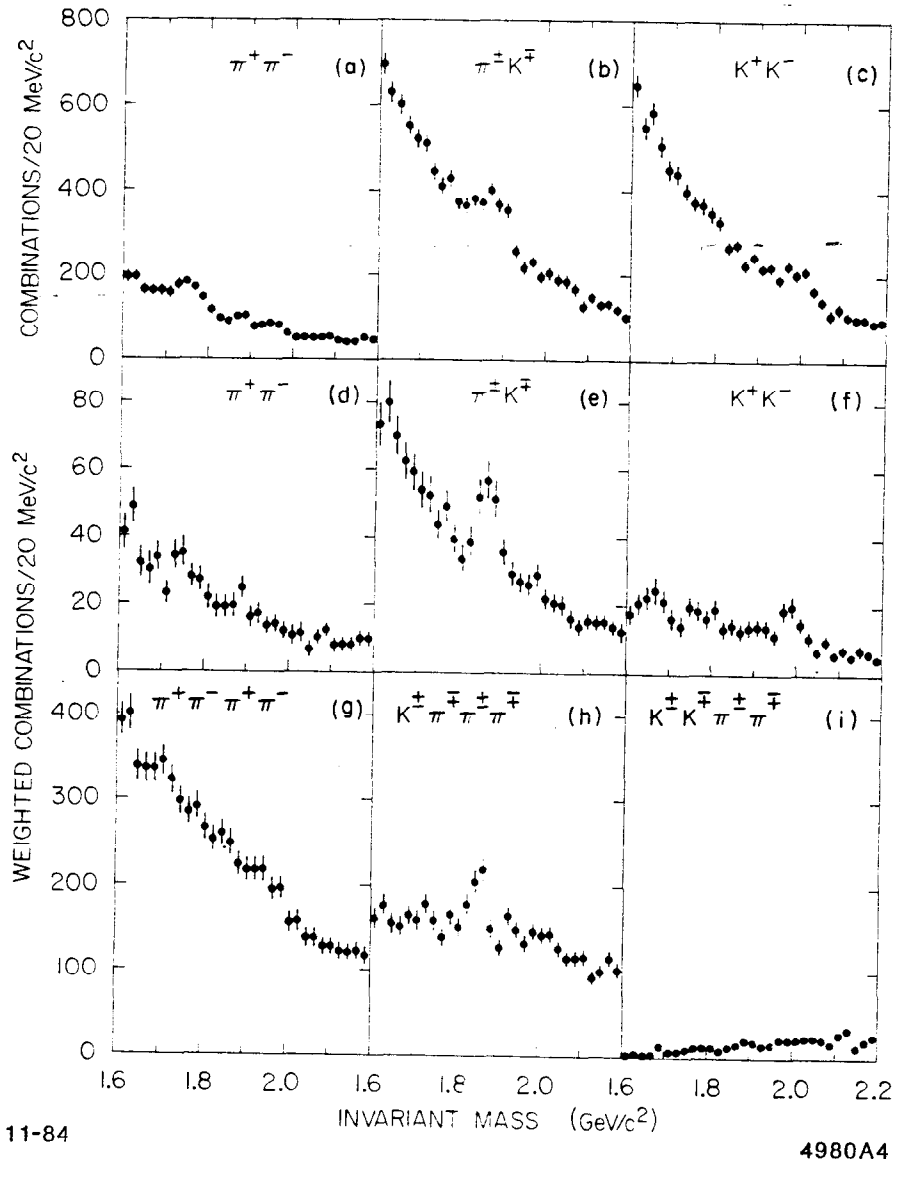

Fig. 4. Observation of exclusive decays of charmed mesons. Shown are invariant mass spectra for neutral combinations of charged particles. (a) $\pi^+\pi^-$ assigning π mass to all tracks, (b) $K^\mp\pi^\pm$ assigning K and π masses to all tracks, (c) K^+K^- assigning K mass to all tracks, (d) $\pi^+\pi^-$ weighted by $\pi\pi$ TOF probability, (e) $K^\pm\pi^\pm$ weighted by $K\pi$ TOF probability, (f) K^+K^- weighted by KK TOF probability, (g) $\pi^+\pi^-\pi^+\pi^-$ weighted by 4π TOF probability, (h) $K^\pm\pi^\mp\pi^\pm\pi^\mp$ weighted by $K3\pi$ TOF probability, (i) $K^+K^-\pi^+\pi^-$ weighted by $KK\pi\pi$ TOF probability.

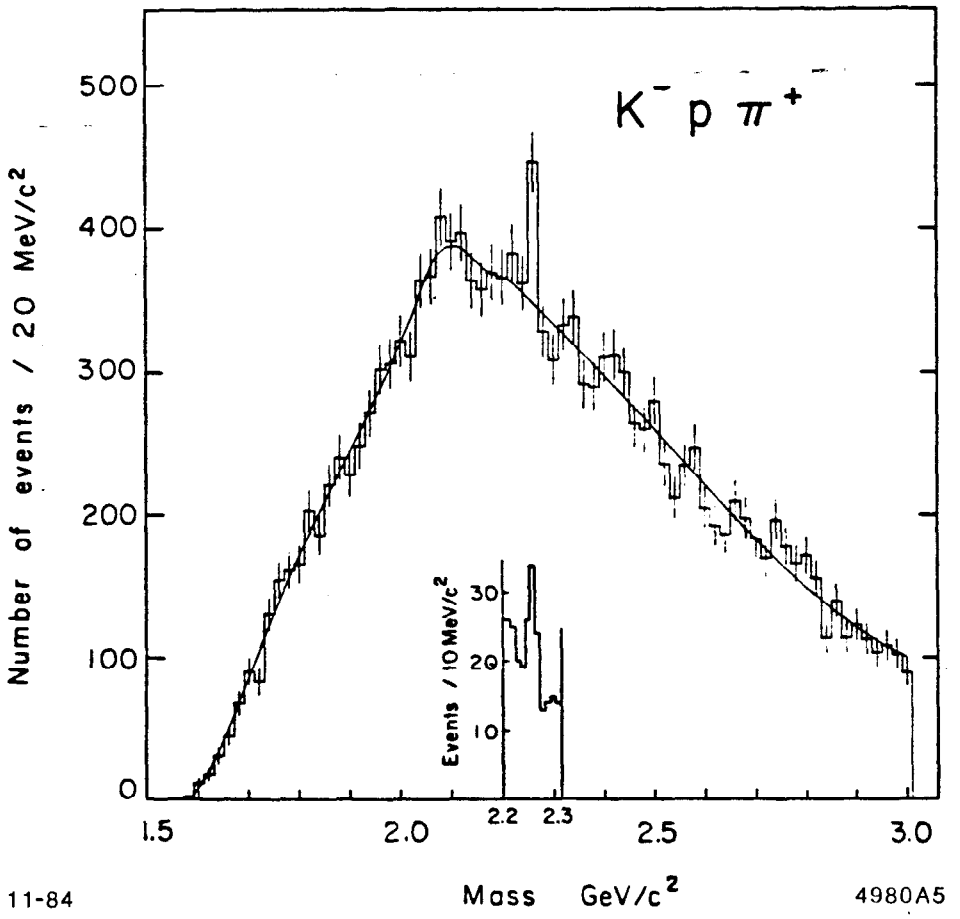

Fig. 5. The charmed baryon is observed in pp collisions at the ISR. Plotted is the invariant mass for $K^-p\pi^+$ combinations. There is a five standard deviation peak above a polynomial background. The inset shows a subset of the data where the resolution was better.

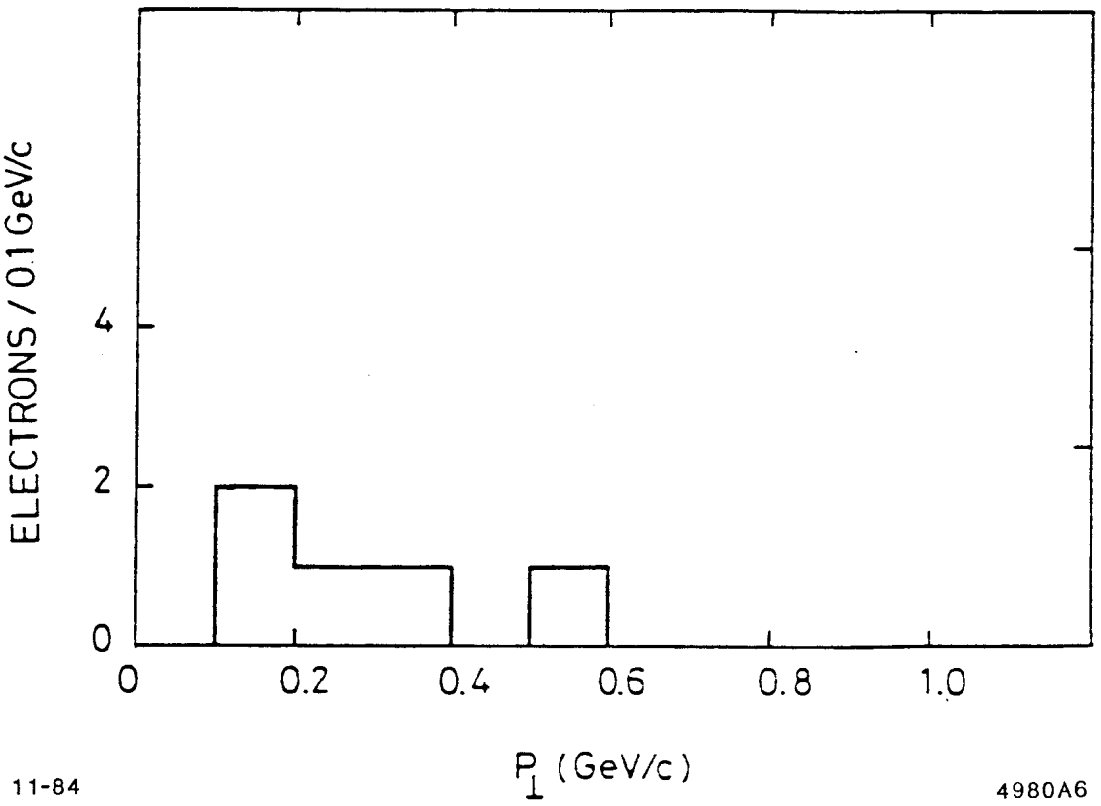

Fig. 6. Transverse momentum spectrum of direct single electrons produced in $\pi^- p$ interactions. These electrons presumably came from semileptonic charm decays.

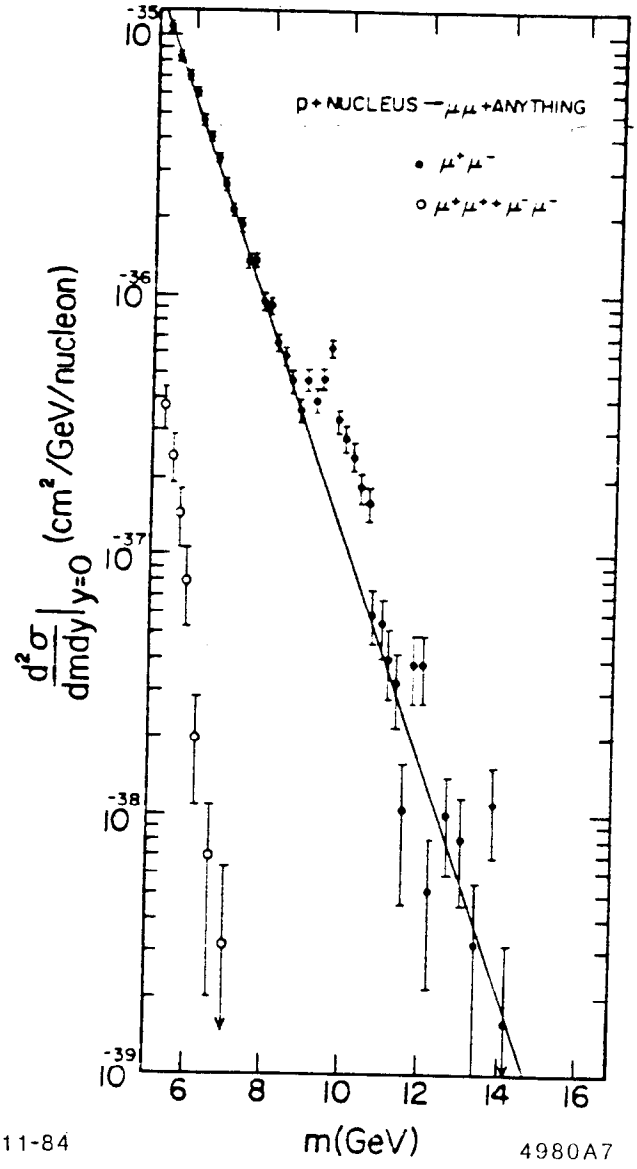

Fig. 7. Observation of the Υ in p + *nucleus* $\rightarrow \mu^+\mu^- X$. The measured dimuon production cross section is plotted as a function of the invariant mass of the muon pair.

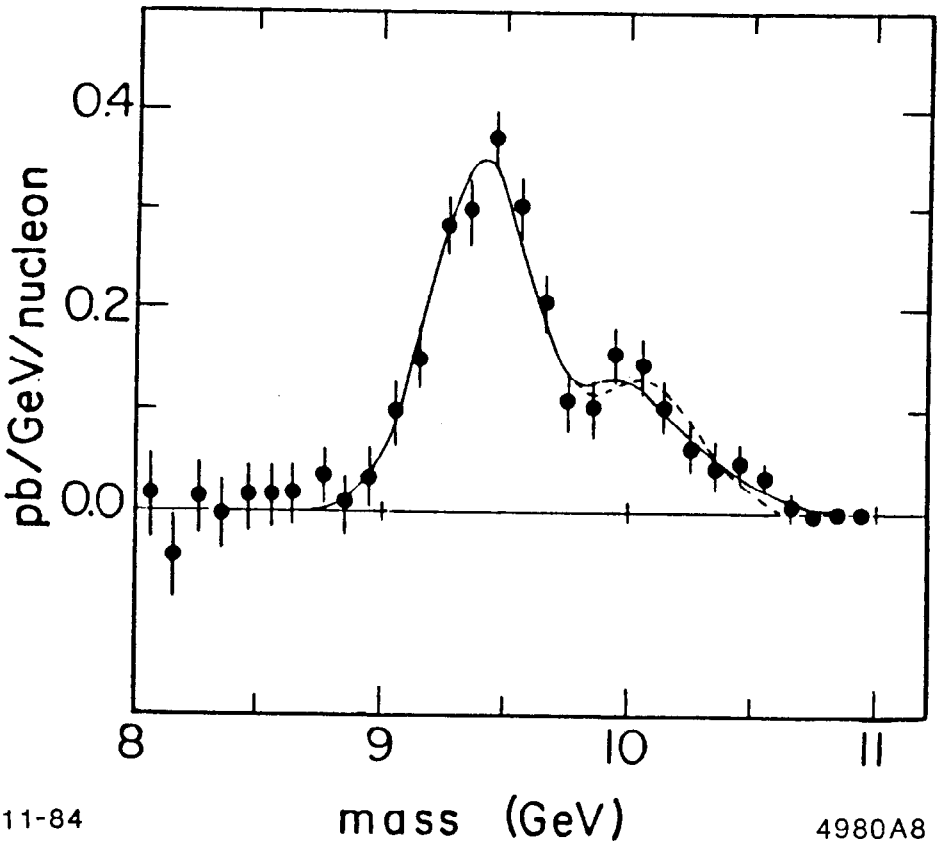

Fig. 8. Details of the Υ resonance seen in p + *nucleus* $\rightarrow \mu^+\mu^- X$.

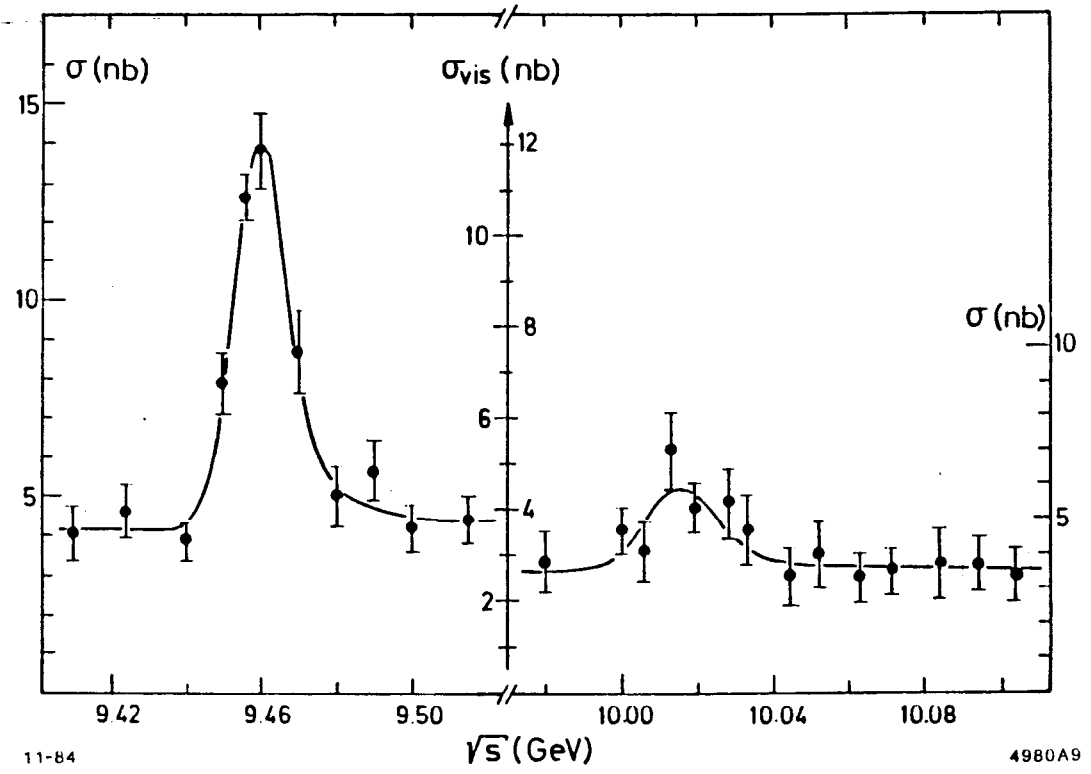

Fig. 9. The $\Upsilon(1S)$ and $\Upsilon(2S)$ seen as peaks in the e^+e^- total cross section.

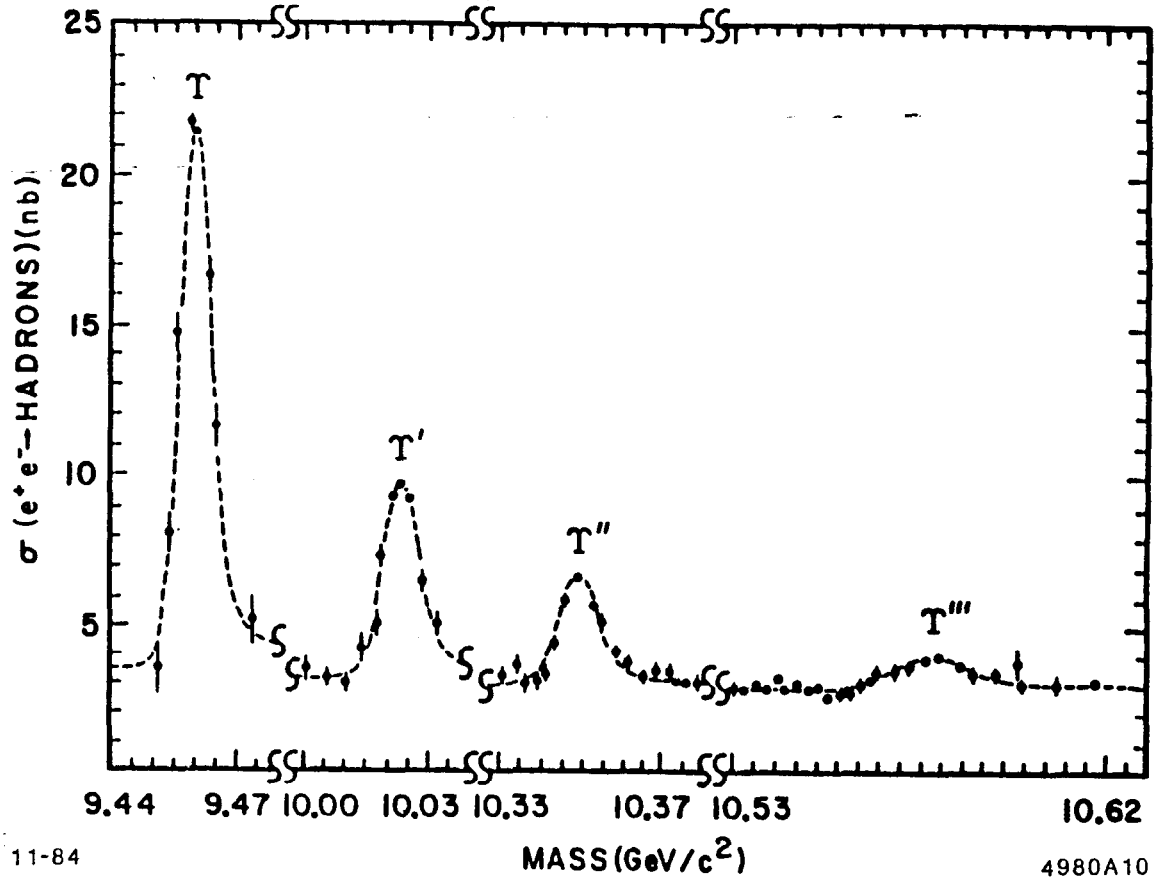

Fig. 10. Four Υ's seen in a plot of e^+e^- cross section as a function of center-of-mass energy.

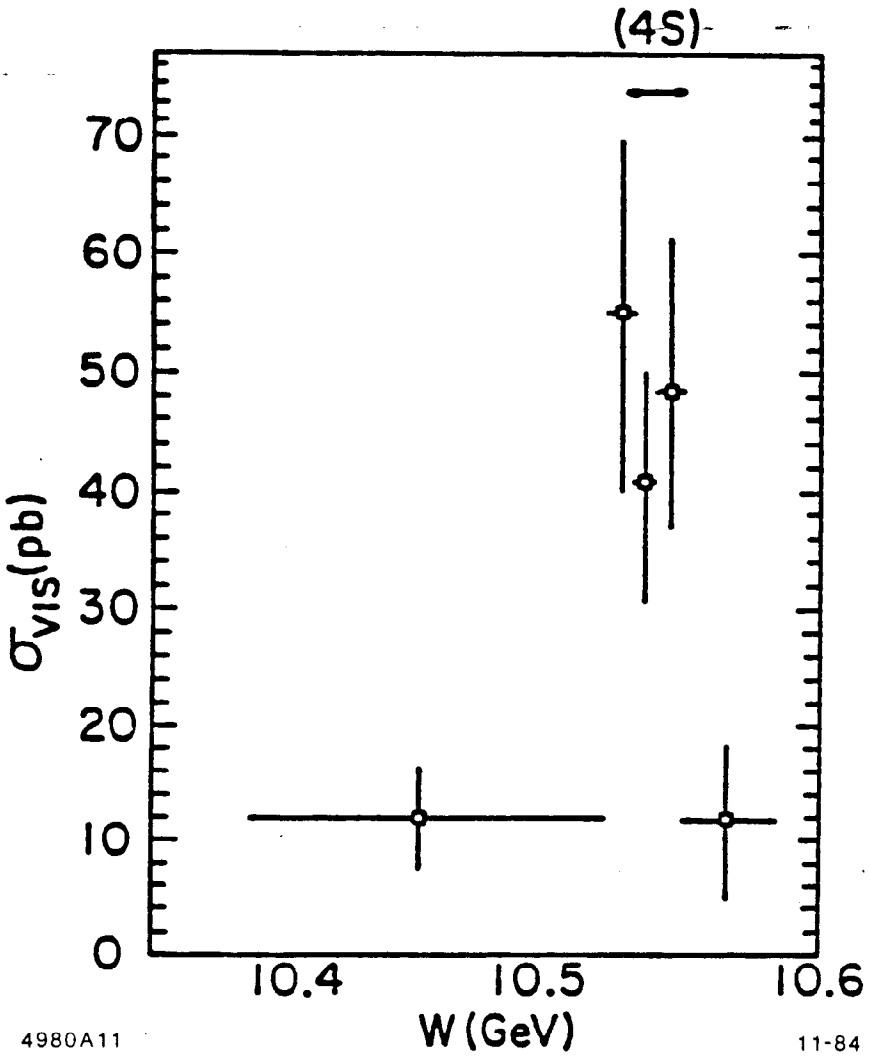

Fig. 11. Electron yield from hadronic events, as a function of center of mass energy. This provides evidence for B meson semileptonic decays.

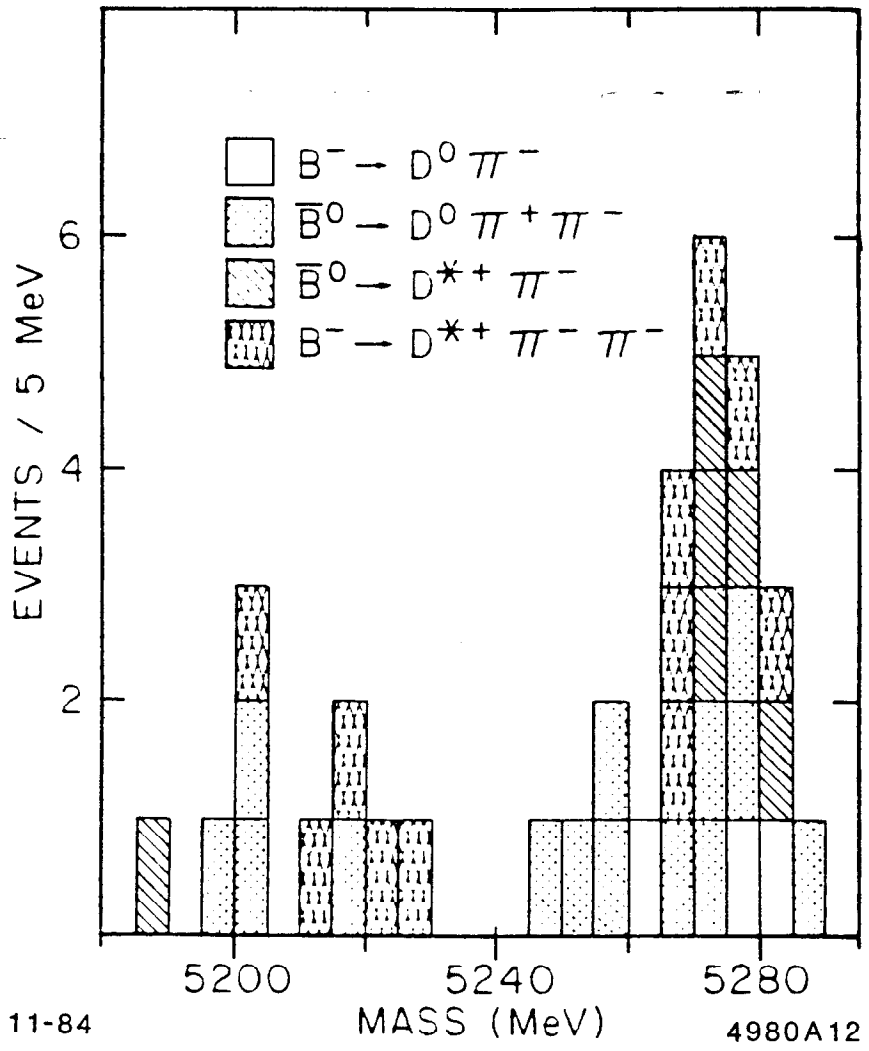

Fig. 12. Observation of exclusive decay modes of B mesons. The mass distribution of B meson candidates is plotted.

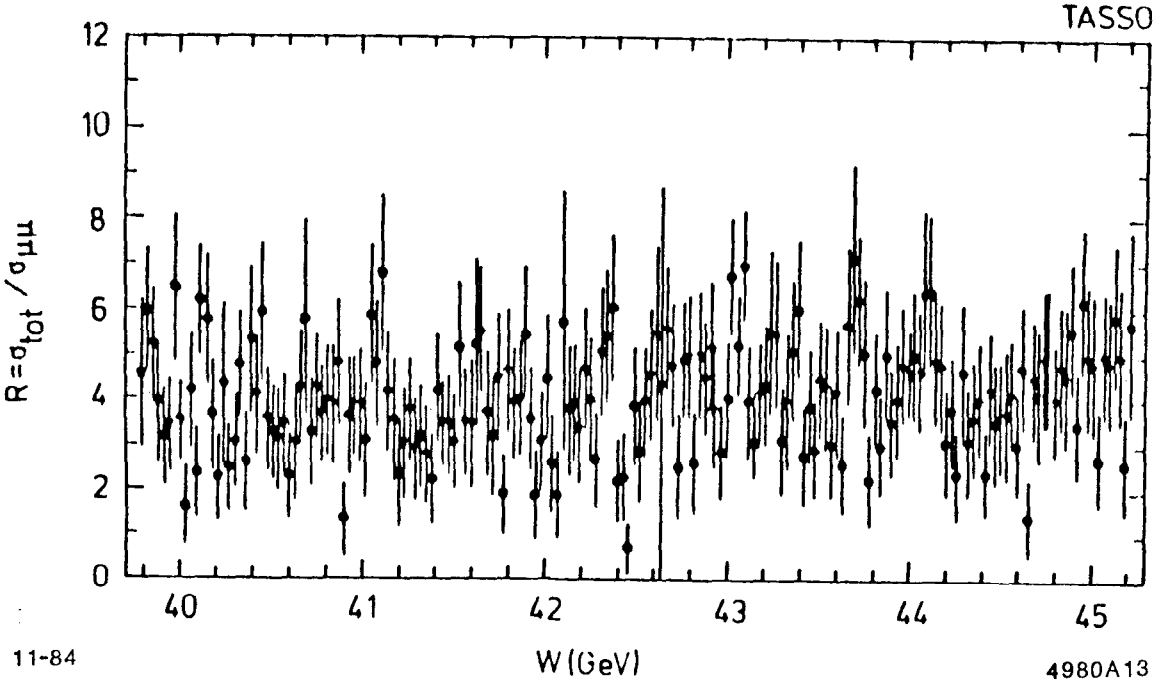

Fig. 13. Cross section measured during an energy scan at PETRA. There is no evidence for a toponium signal.

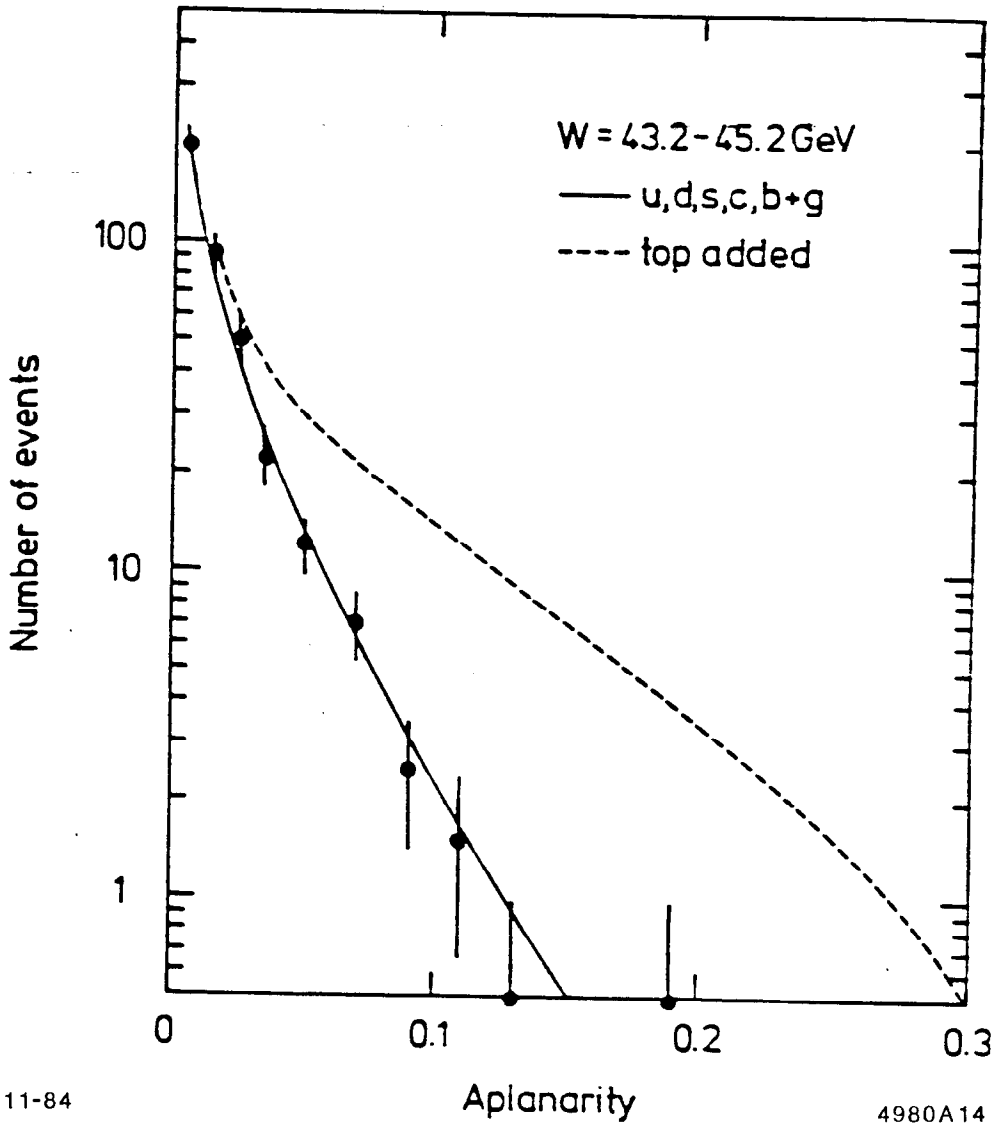

Fig. 14. The aplanarity distribution of events taken by TASSO at the highest PETRA energies. There is no indication of aplanar events as would result from top decay.

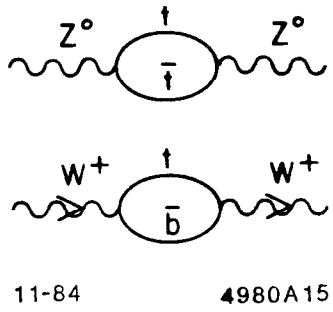

Fig. 15. Mass renormalization diagrams involving the top quark.

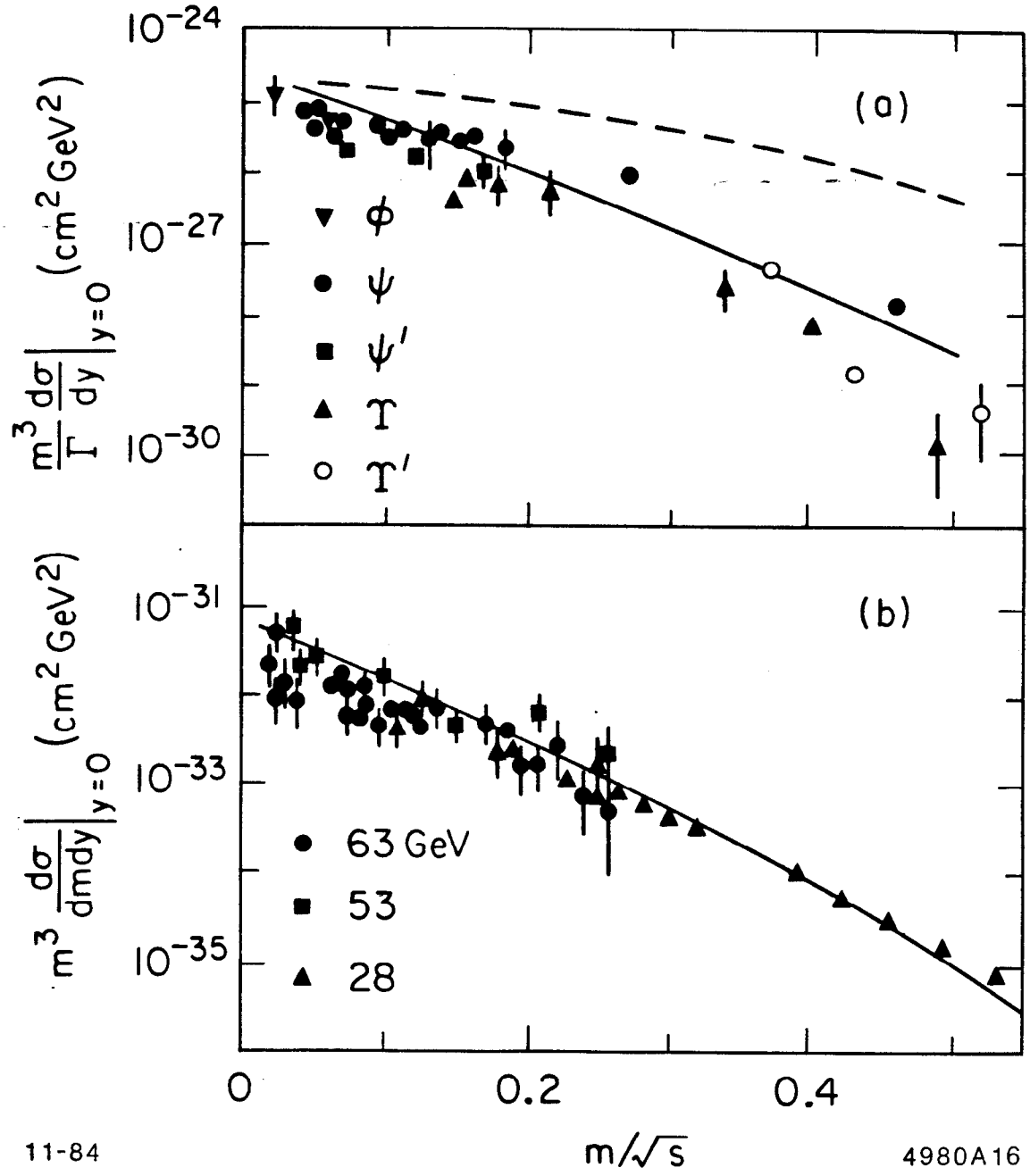

Fig. 16. Scaling laws for (a) vector meson production and (b) Drell-Yan lepton pair production.

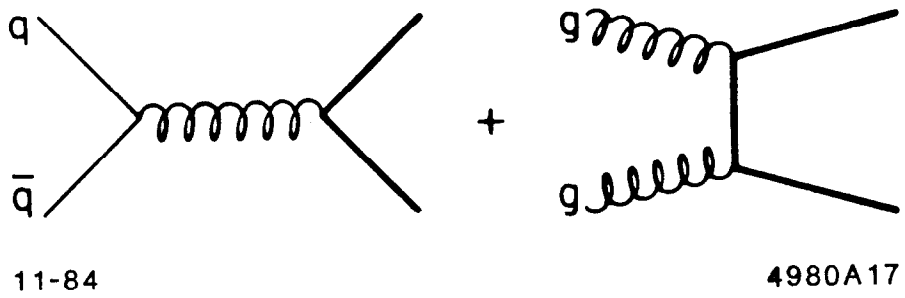

Fig. 17. Lowest order diagrams for strong production of heavy quarks.

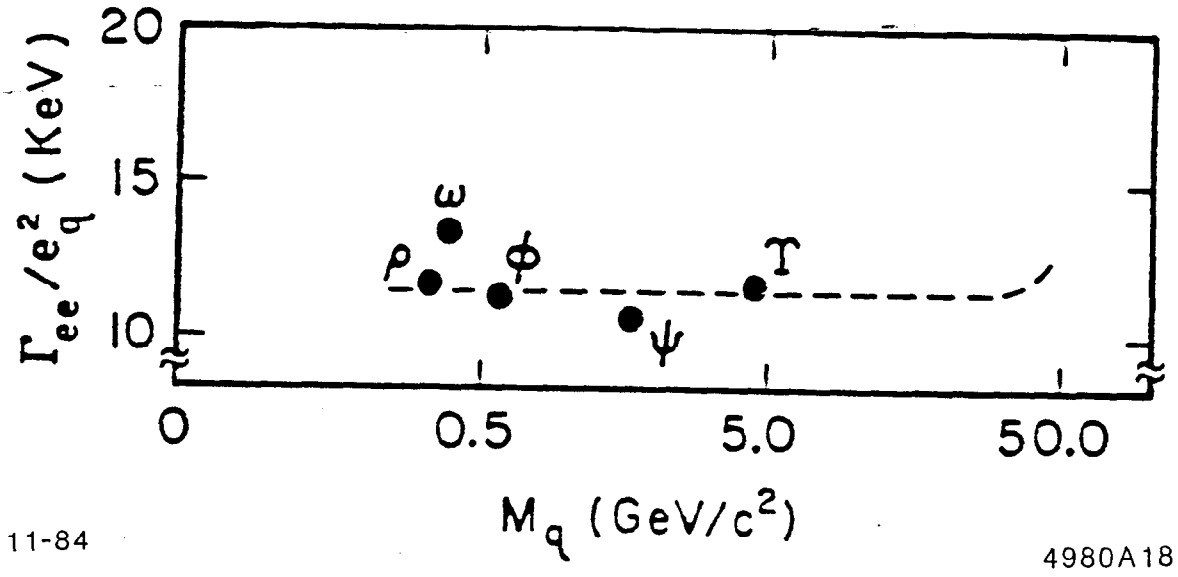

Fig. 18. A scaling law for the leptonic widths of vector mesons.

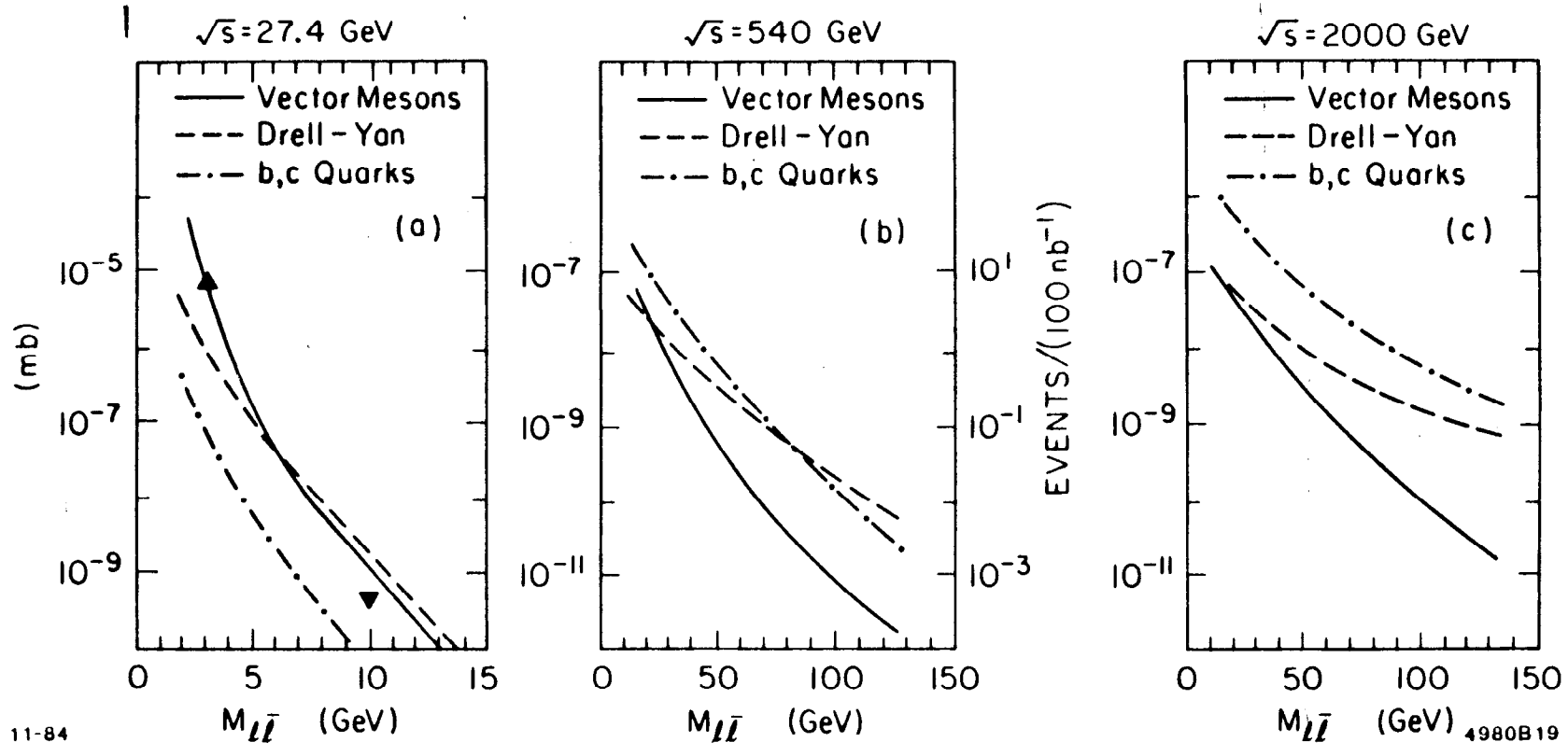

Fig. 19. Proton-Proton production cross sections for lepton pairs scaled from ψ production at the ISR.

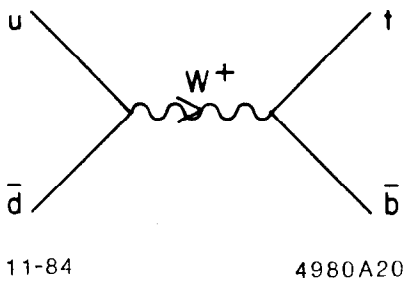

Fig. 20. Diagram to produce $t\bar{b}$ via a W.

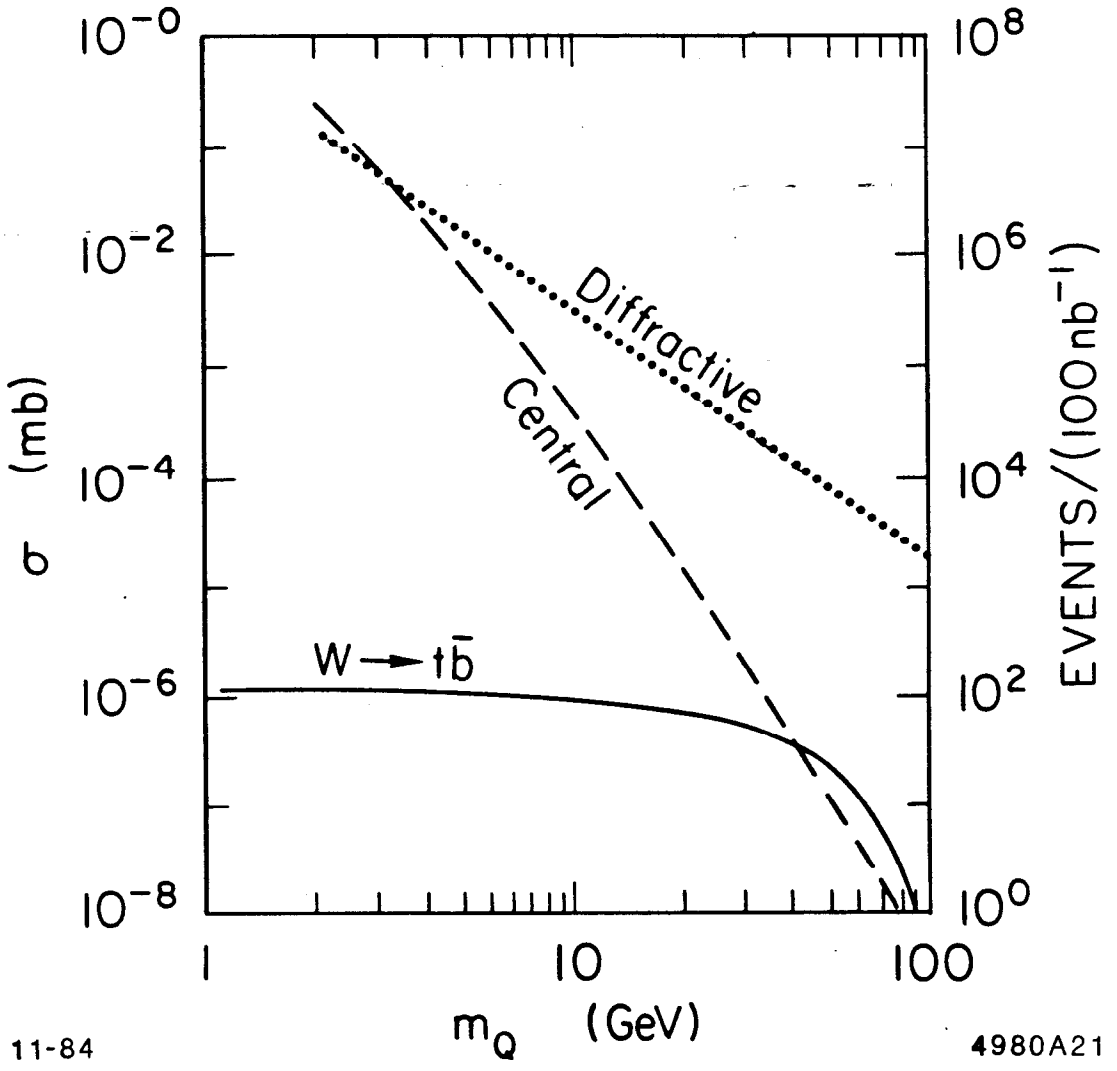

Fig. 21. Heavy quark production cross sections as a function of the heavy quark mass. The 3 different production mechanisms are explained in the text.

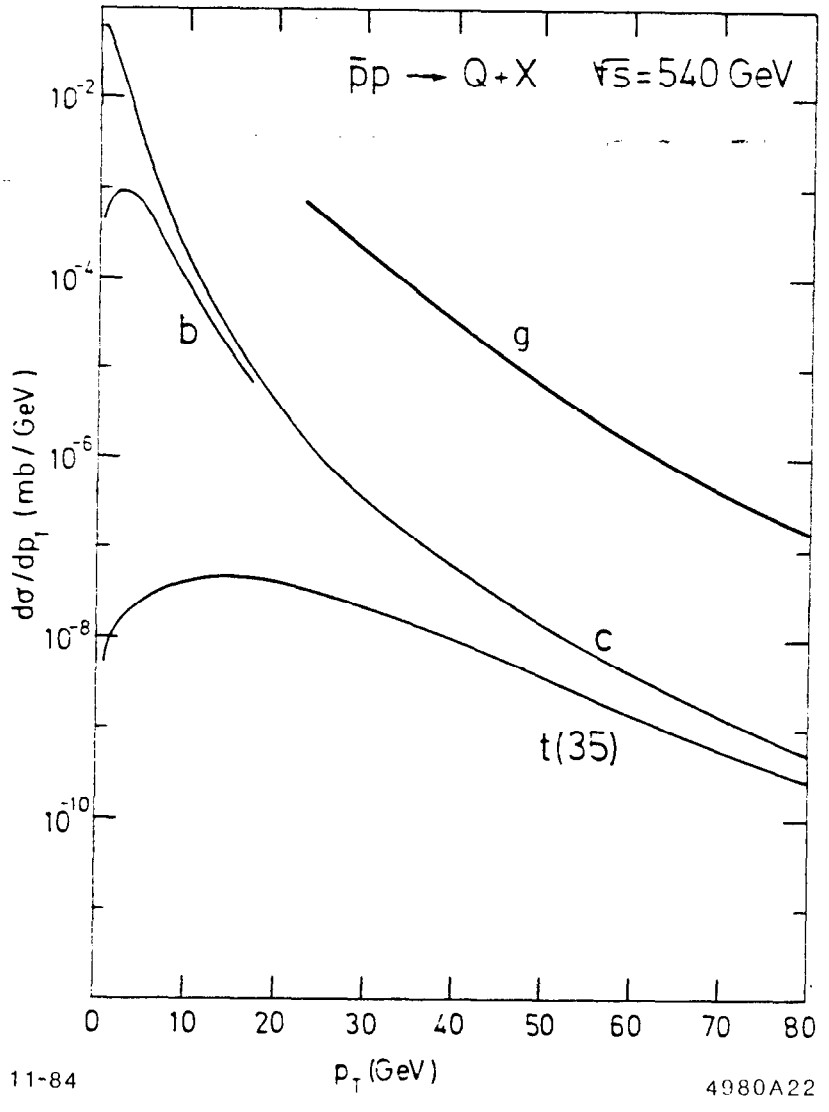

Fig. 22. Calculated differential cross sections for production of heavy quark or gluon jets.

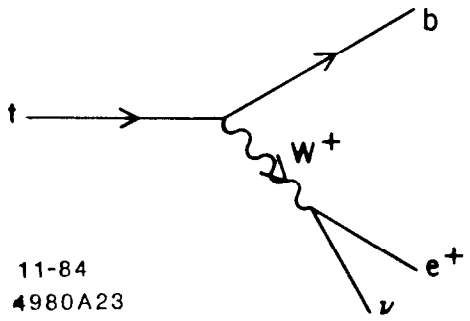

Fig. 23. Diagram for semileptonic decay of top.

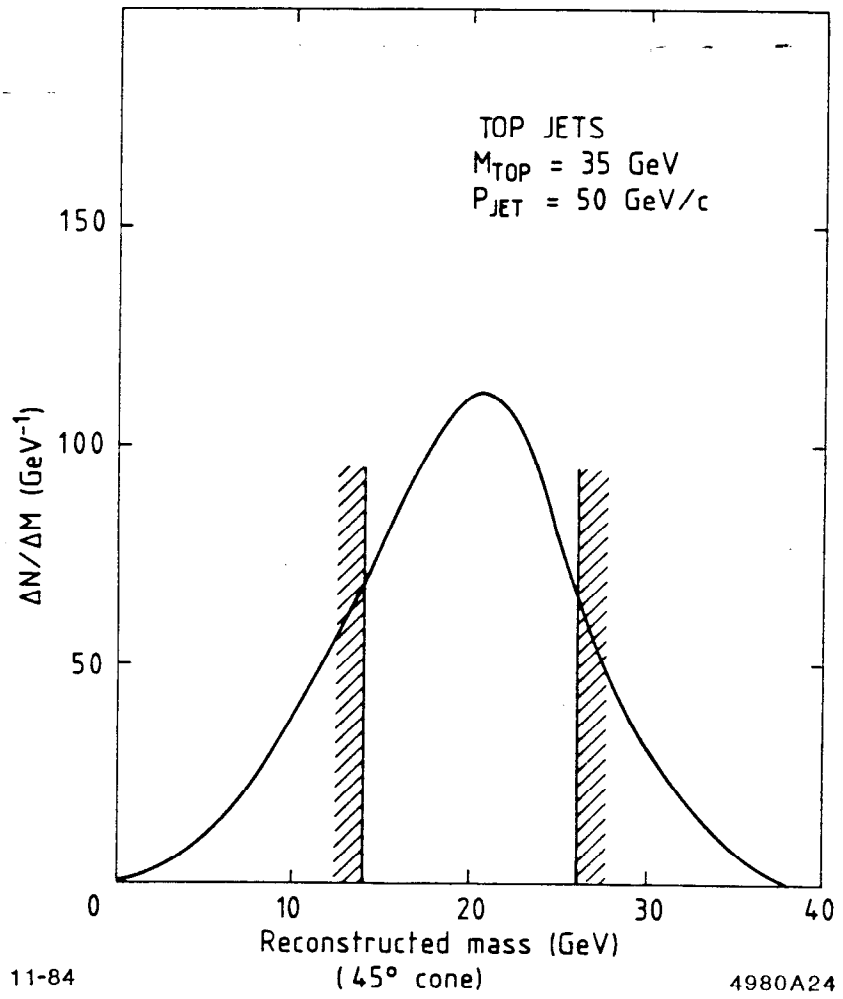

Fig. 24. Distribution of reconstructed jet masses for top jets generated with $m_{top} = 35$ GeV/c^2 and $p_T = 50$ GeV/c.

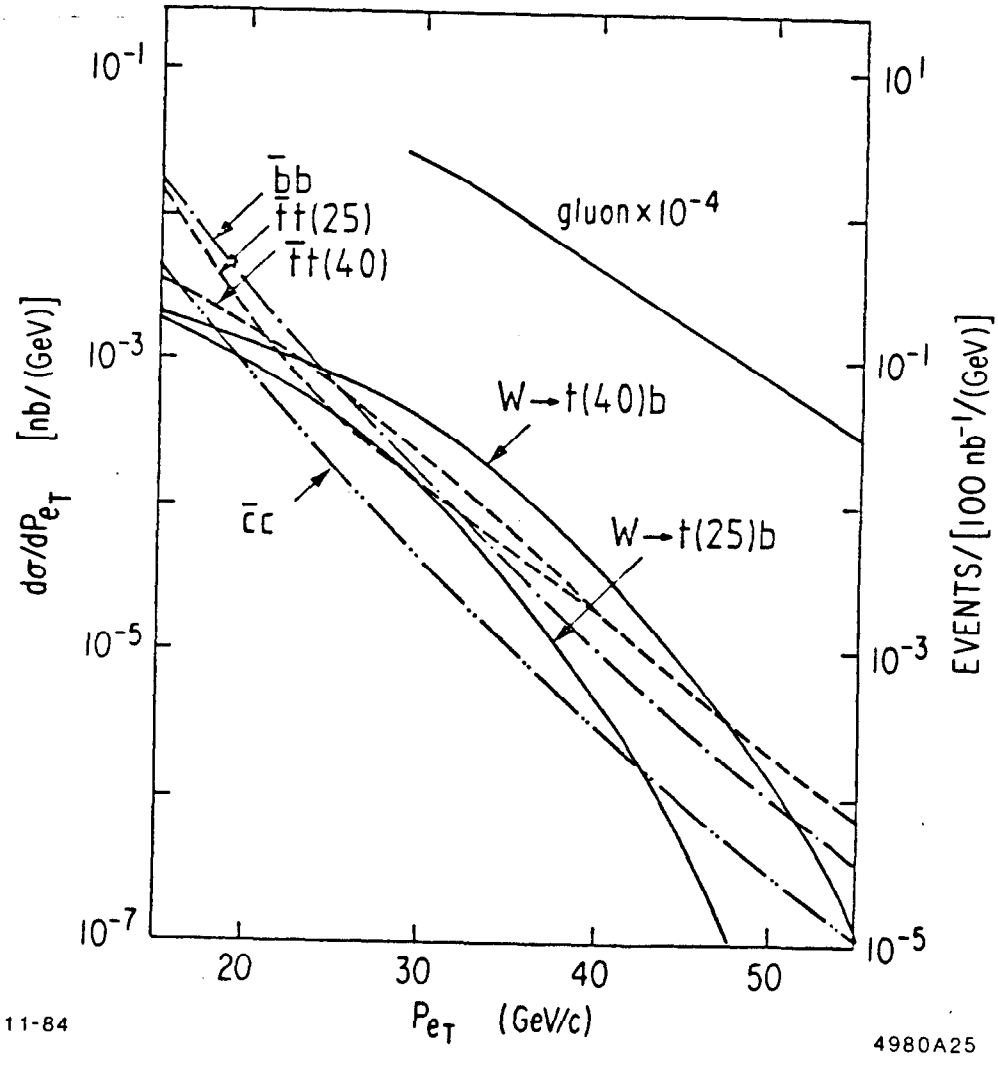

Fig. 25. Momentum spectra of electrons coming from t decay and from background sources.

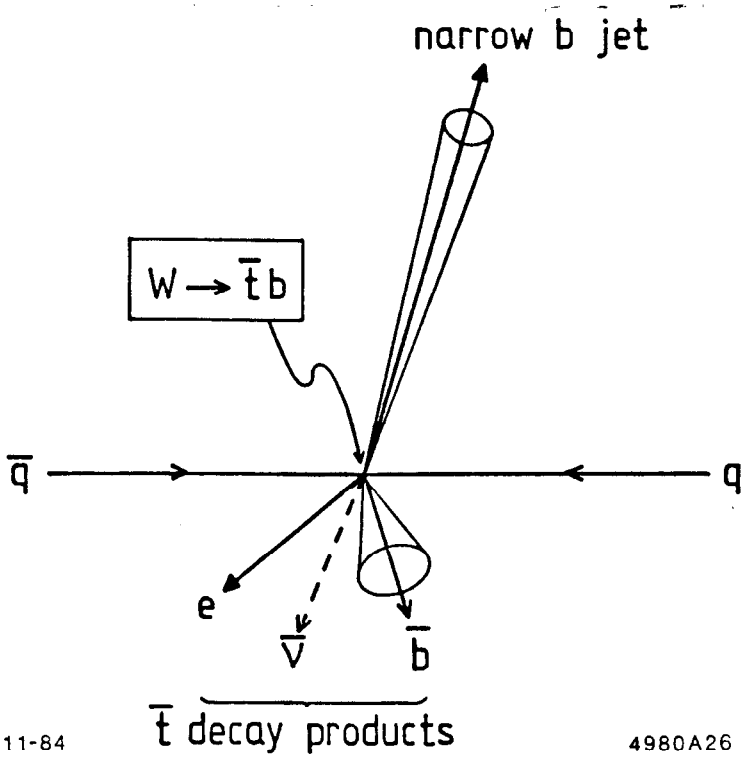

Fig. 26. Sketch of an event where $W \to \bar{t}b$ and the $\bar{t}$ decays semileptonically.

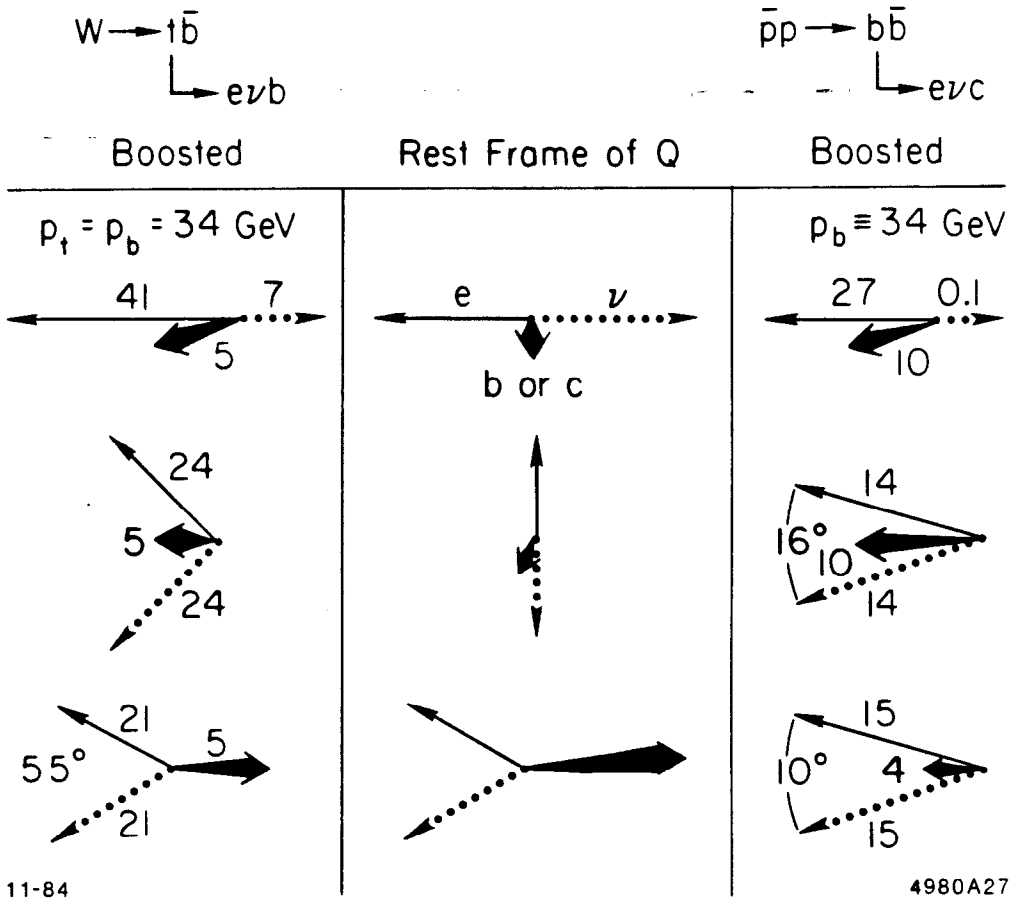

Fig. 27. Kinematic examples of $W \to t\bar{b}$ and $p\bar{p} \to b\bar{b}$ where the t or b decays semileptonically.

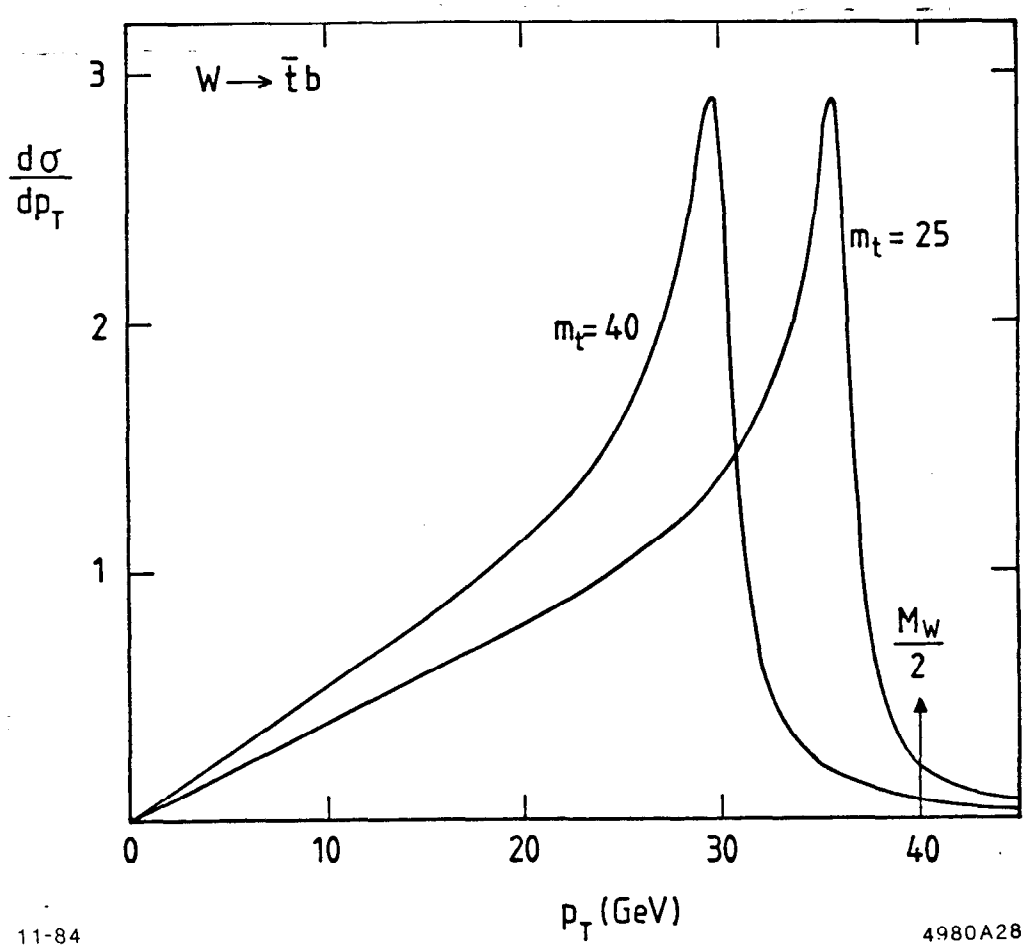

Fig. 28. The Jacobian peak expected in the transverse momentum distribution of the b jet from $W \rightarrow \bar{t}b$ for two different top masses. Effects of detector resolution are not included.

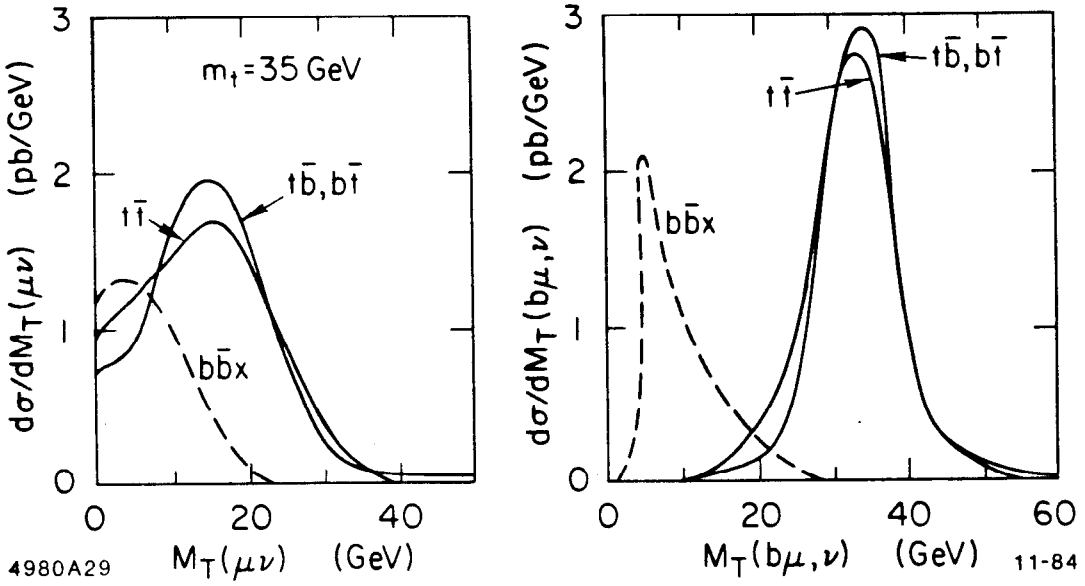

Fig. 29. Calculated transverse mass distributions for $t\bar{t}$, $t\bar{b}$ and $b\bar{b}$ events.

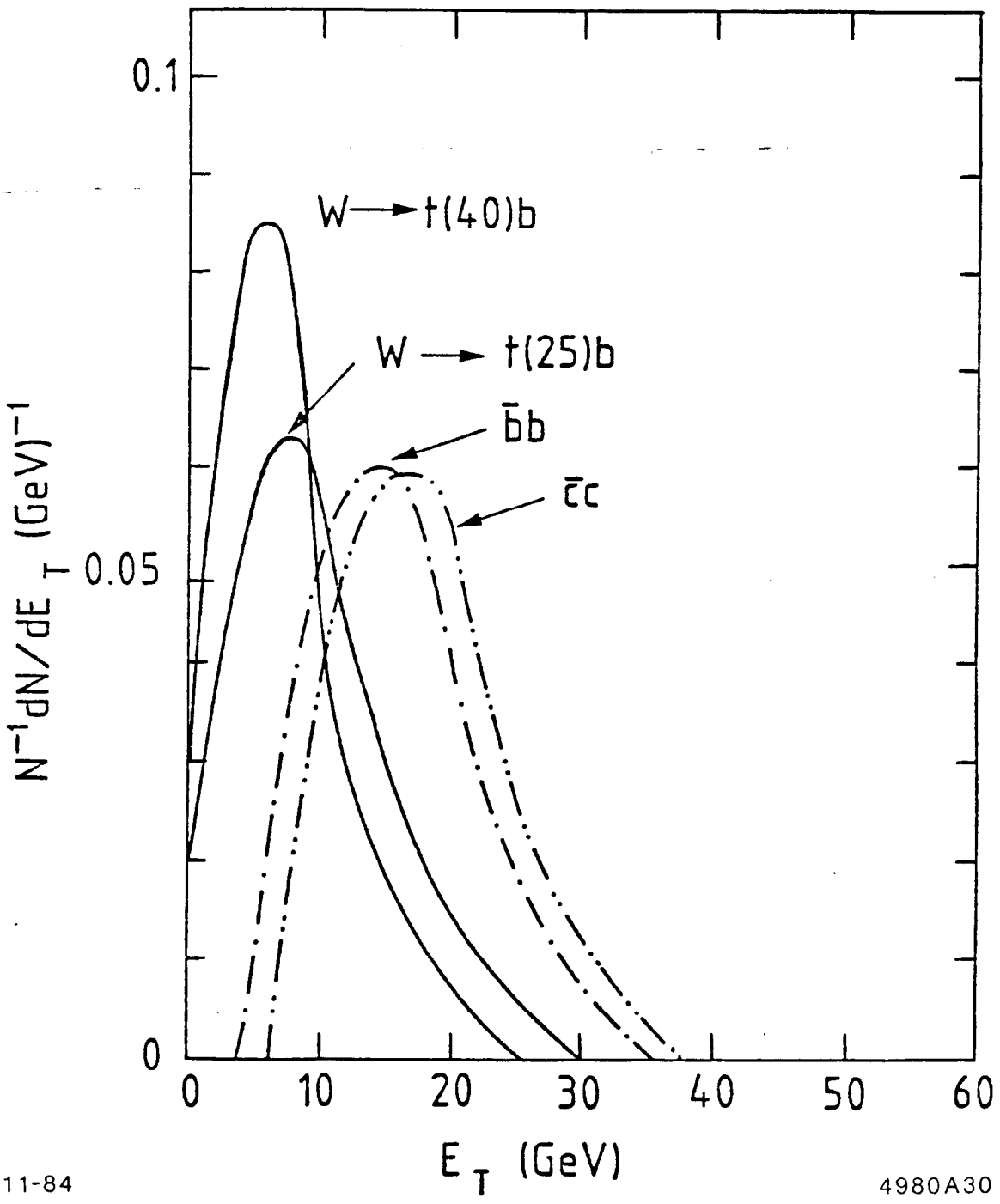

Fig. 30. Calculation of the distribution of hadronic transverse energy deposited within ±30° in azimuth of the electron. Top decays have less nearby energy than *b* or *c* decays.

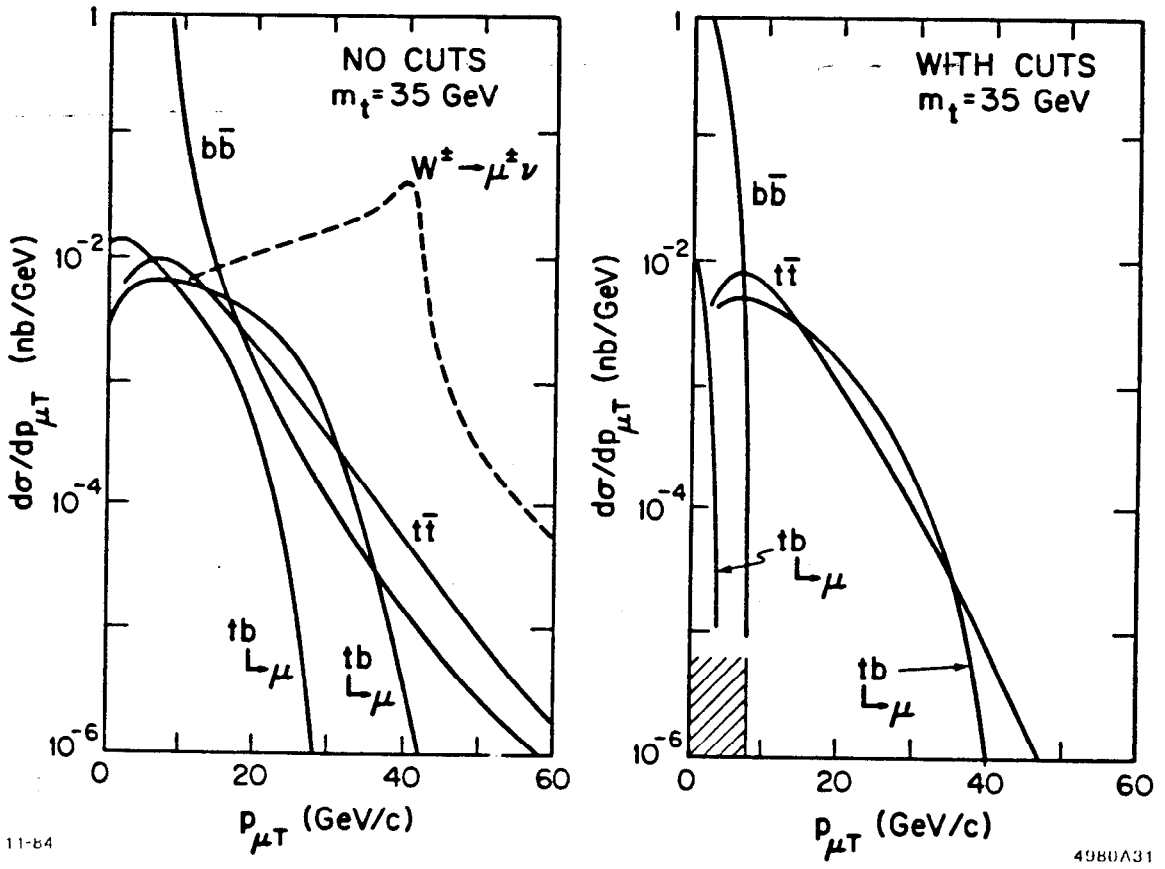

Fig. 31. Calculated p_T distribution of leptons from various sources. Gluon bremsstrahlung was not included in the calculation.

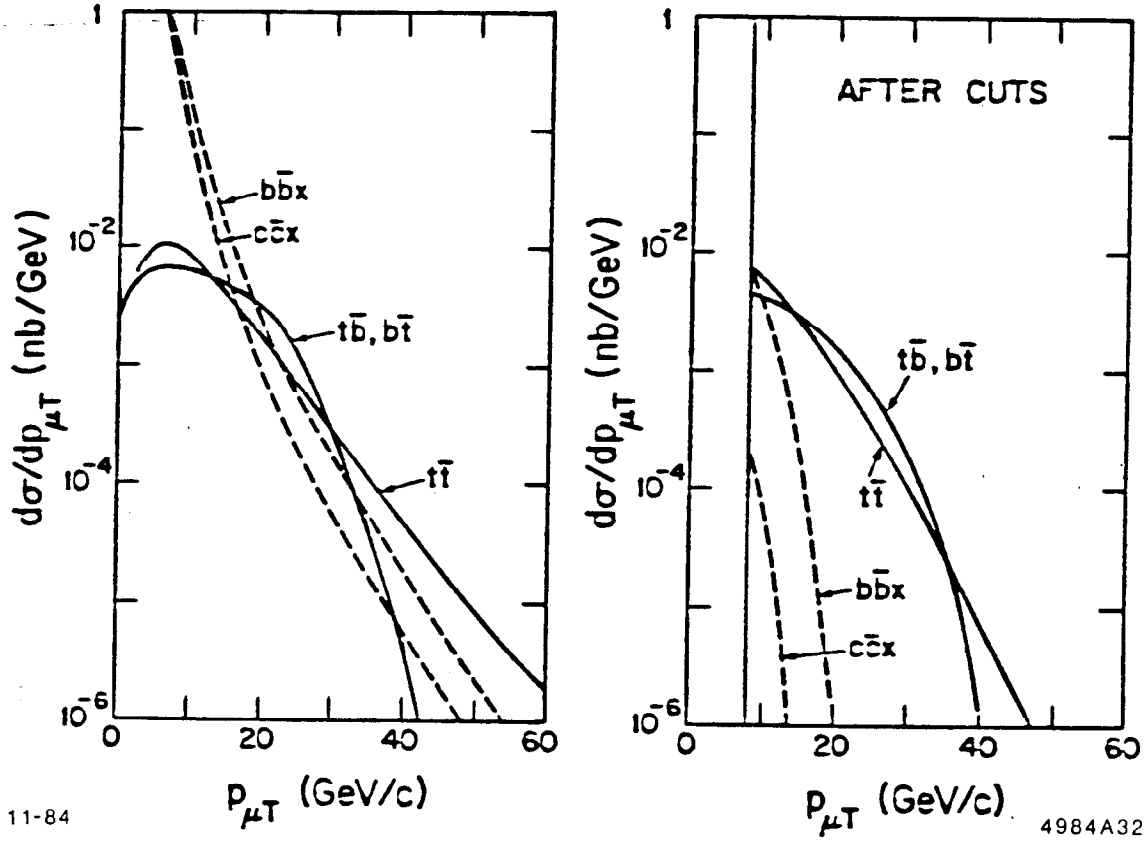

Fig. 32. Calculated p_T distribution of leptons from various sources. Gluon bremsstrahlung was included in the calculation.

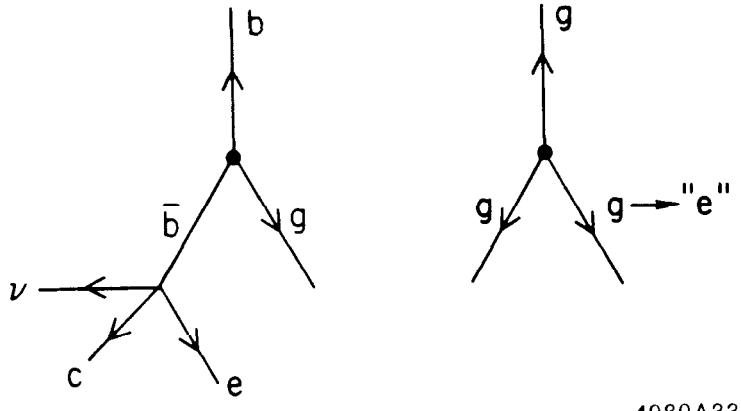

Fig. 33. Comparison of how a $b\bar{b}$ event and a gg event can simulate a top event. Both need a gluon bremsstrahlung.

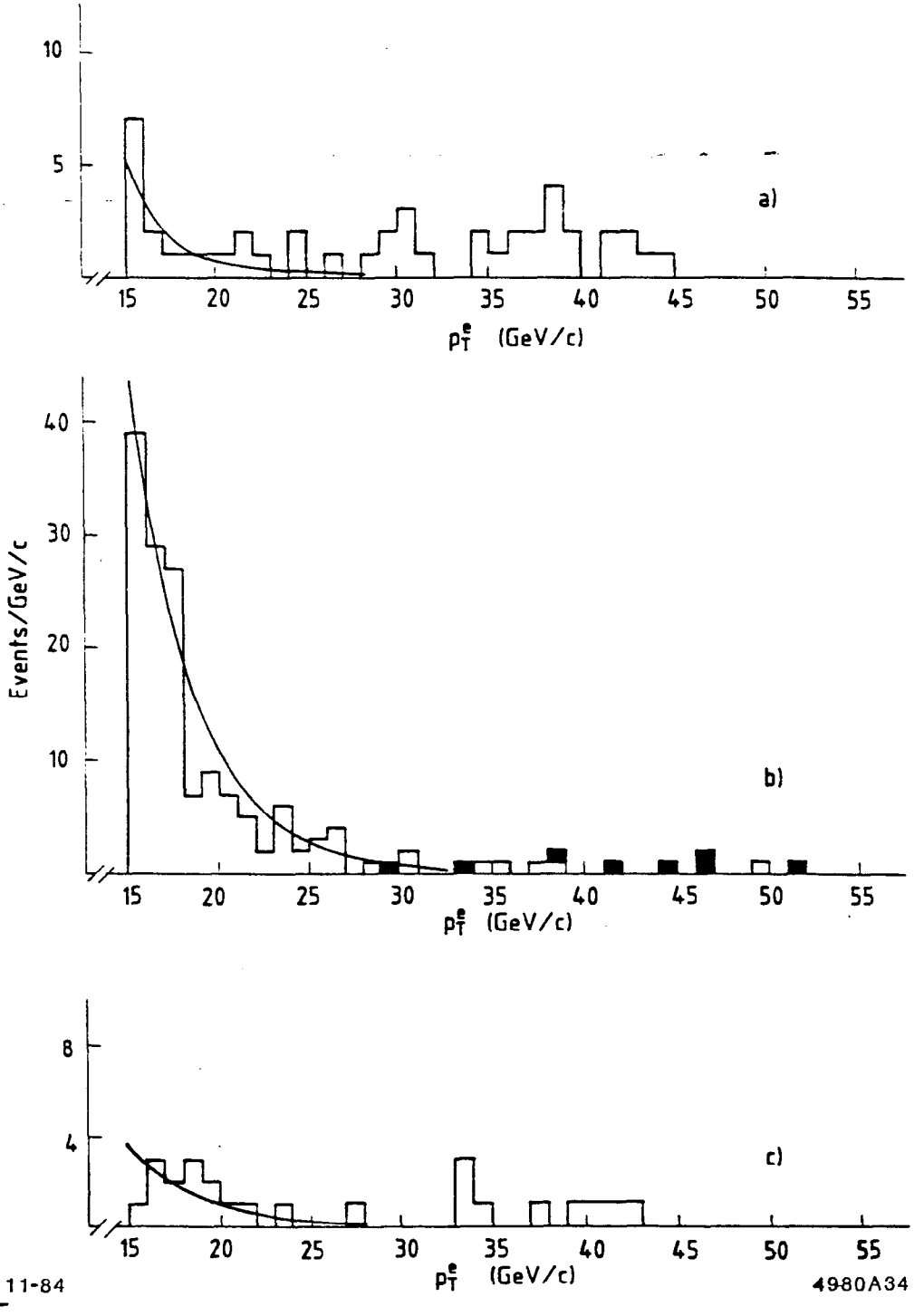

Fig. 34. Transverse momentum distribution of the electron candidates in events with: (a) no additional jets, (b) with a jet opposite the electron, (c) with a jet which isn't opposite the electron. The dark areas correspond to the eight Z° events.

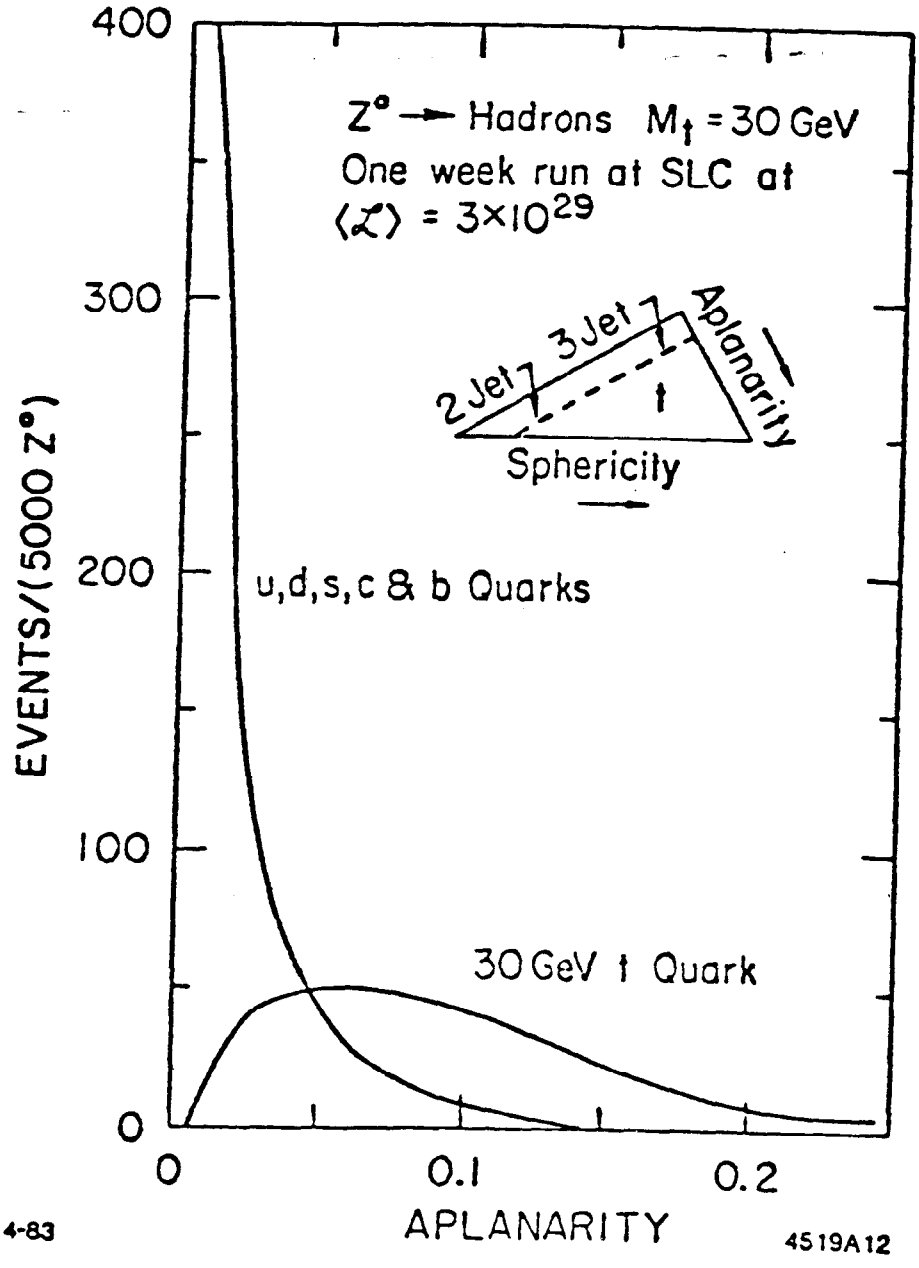

Fig. 35. Expected aplanarity distribution for light quarks and a 30 GeV/c^2 top quark.

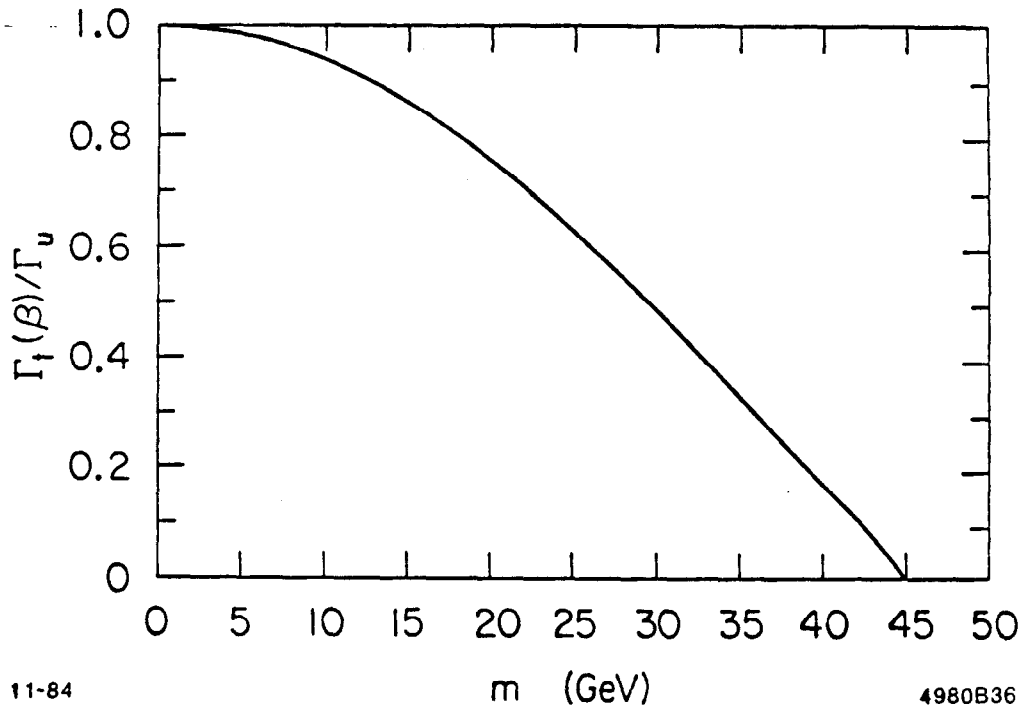

Fig. 36. Branching ratio for $Z^\circ \to t\bar{t}$ relative to Z° decay to a light quark pair.

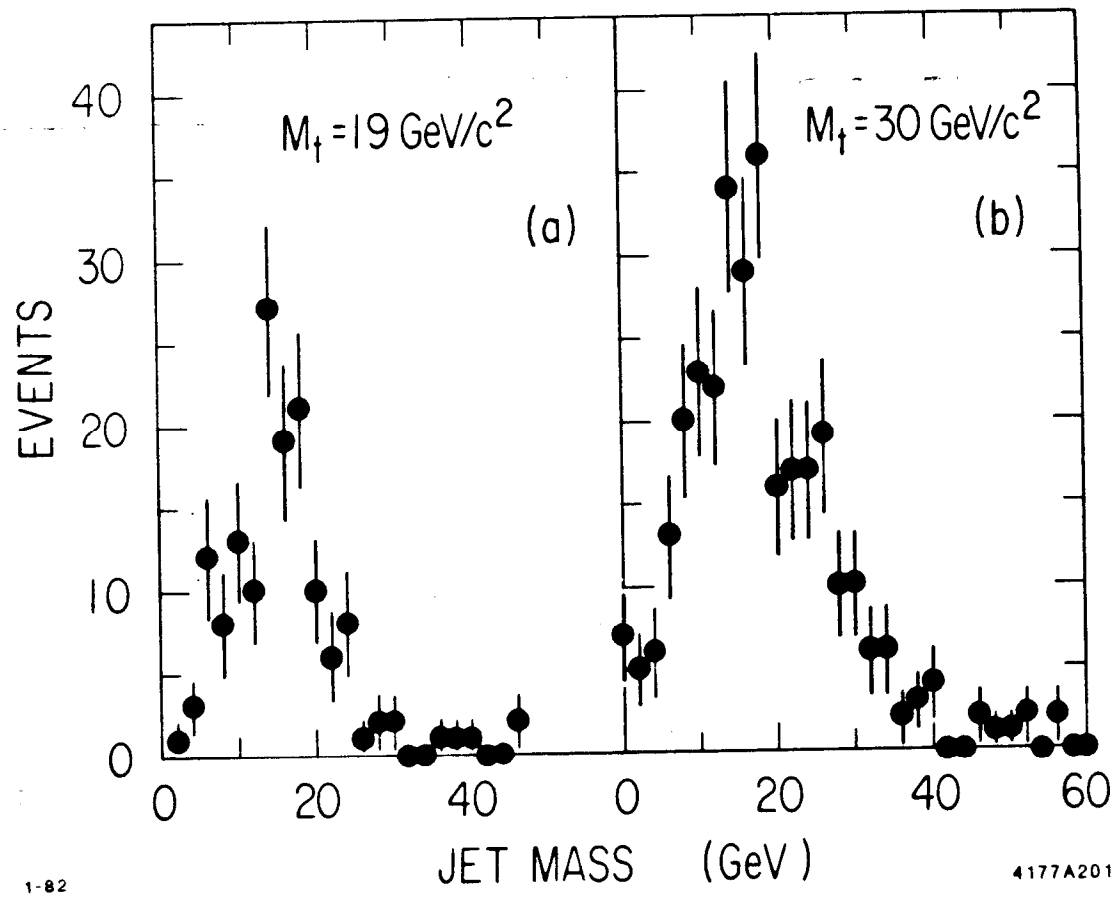

Fig. 37. Reconstructed jet masses for two different top quark masses.

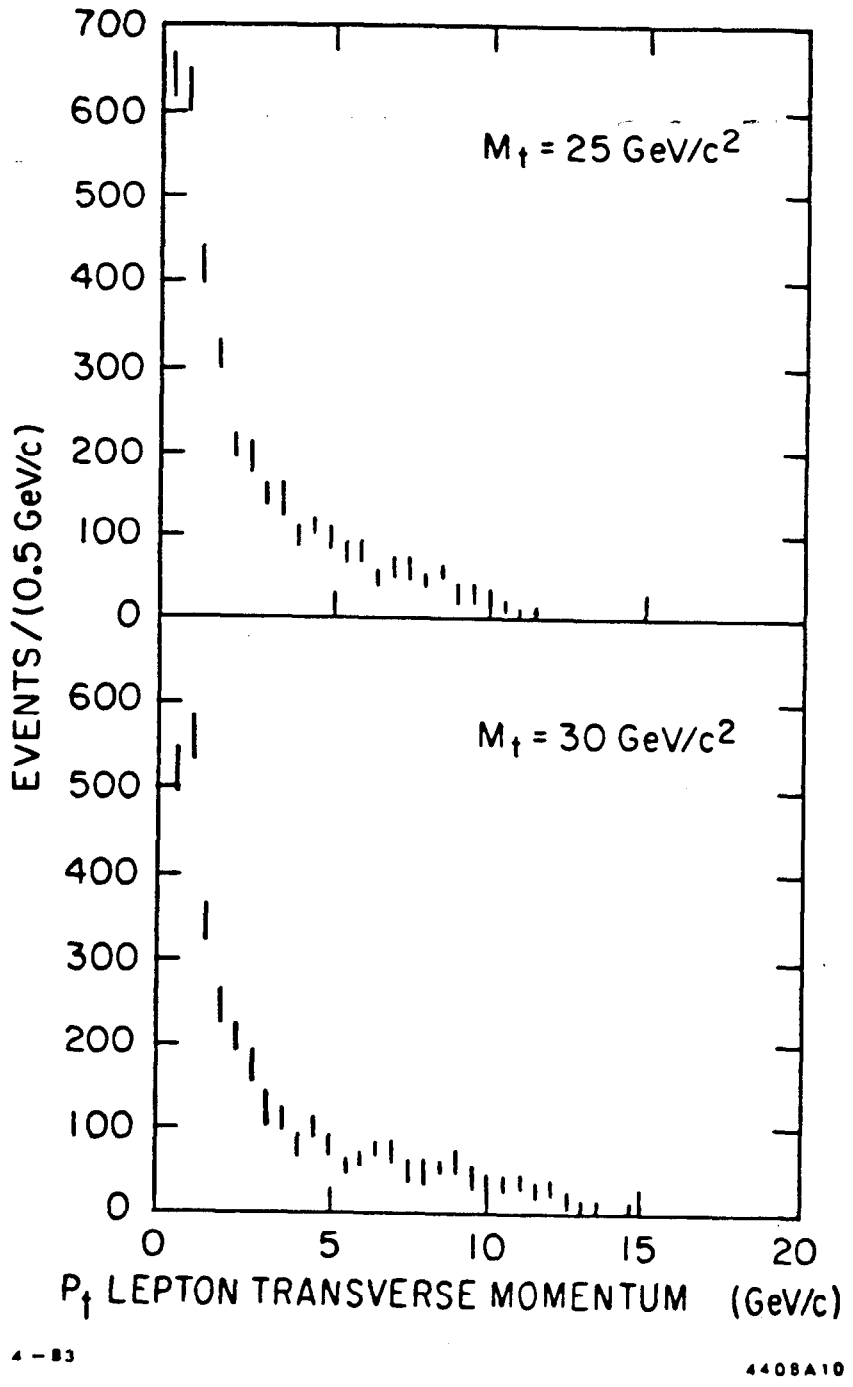

Fig. 38. Monte Carlo calculations of the distribution of lepton momenta transverse to the jet direction. The endpoint determines the mass of the top quark.

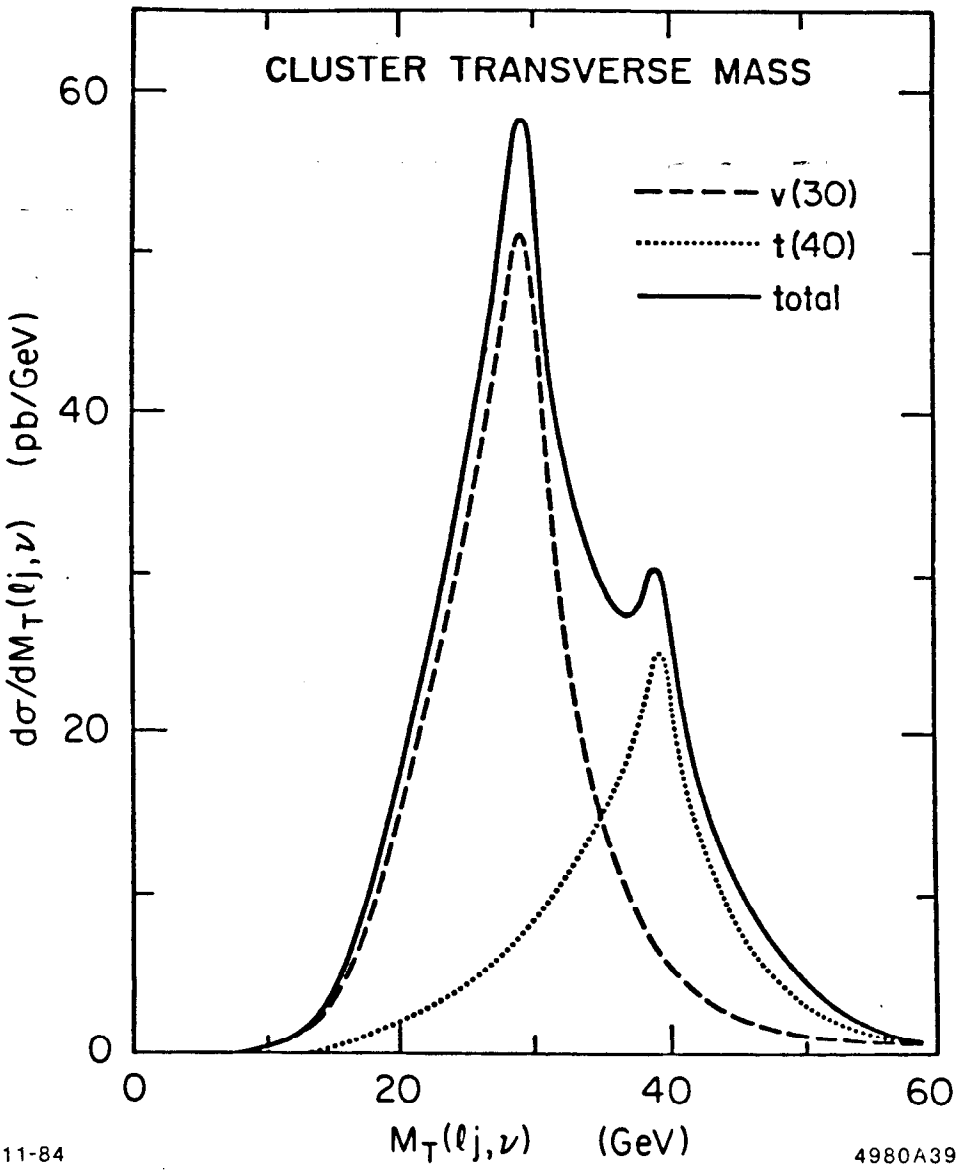

Fig. 39. Expected transverse mass spectrum for the case with a 30 GeV/c^2 charge 1/3 quark and a 40 GeV/c^2 charge 2/3 quark.

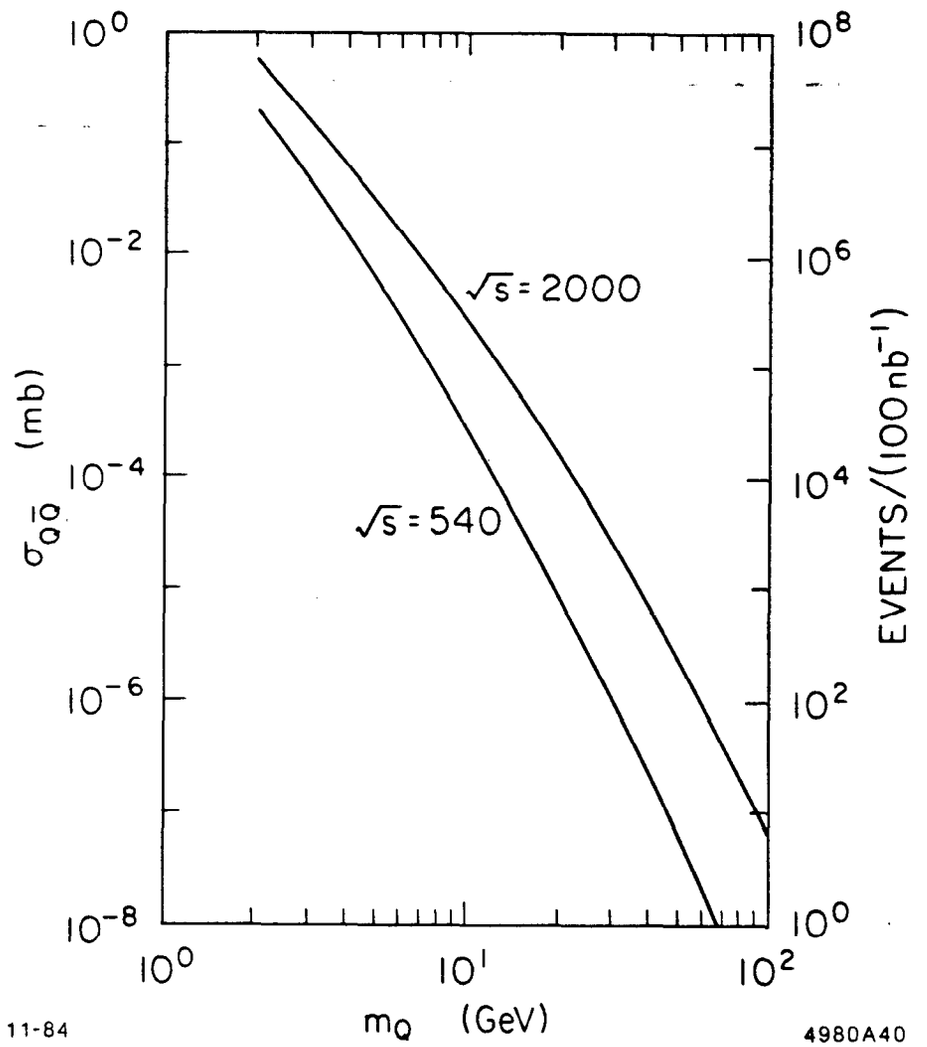

Fig. 40. Calculated production cross sections for heavy quarks as a function of the quark mass.